

EVALUATION OF ENERGY RELEASE FROM WILDFIRES ACROSS THE  
ELEVATION GRADIENT

by

Isabelle Rose Butler



A thesis

submitted in partial fulfillment

of the requirements for the degree of

Master of Science in Civil Engineering

Boise State University

August 2022

© 2022

Isabelle Rose Butler

ALL RIGHTS RESERVED

BOISE STATE UNIVERSITY GRADUATE COLLEGE

**DEFENSE COMMITTEE AND FINAL READING APPROVALS**

of the thesis submitted by

Isabelle Rose Butler

Thesis Title: Evaluation of Energy Release from Wildfires across the Elevation Gradient

Date of Final Oral Examination: 14 June 2022

The following individuals read and discussed the thesis submitted by student Isabelle Rose Butler and they evaluated her presentation and response to questions during the final oral examination. They found that the student passed the final oral examination.

Mojtaba Sadegh, Ph.D. Chair, Supervisory Committee

Hans-Peter Marshall, Ph.D. Member, Supervisory Committee

Kevin Roche, Ph.D. Member, Supervisory Committee

The final reading approval of the thesis was granted by Mojtaba Sadegh, Ph.D., Chair of the Supervisory Committee. The thesis was approved by the Graduate College.

## DEDICATION

To my family, for their unconditional love, endless support, and good cookin'.

## ACKNOWLEDGEMENTS

First and foremost, my deepest gratitude goes to my advisor, Dr. Mojtaba (Moji) Sadegh, for your encouragement, willingness to share all you know, and patience in answering my questions - twice over. You are the backbone of this thesis no matter how many times you deny it. Thank you, Dr. Kevin Roche, for your wealth of knowledge and contagious enthusiasm for all things water resources, which motivated me more times that I can count. And to you, Dr. HP Marshall; your curiosity inspired my own, and your wealth of knowledge is as diverse as your beloved snow crystals you so willingly put aside to learn about my world of fire.

I'd like to thank the SENS GPS program for providing me the opportunity to complete my Master's degree, and gifting me a community of like-minded individuals full of spunk and determination to look to for guidance. The faculty at Boise State is truly like no other, and I feel privileged to have gotten to know, learned under, and now be able to thank them for their continuous support over the years.

Thank you to the friends I have made during this journey and those who have been there since the beginning, to Gavin for your love, support, and telling me how smart I am so often I eventually believed it myself, and last but not least, my family. You have my most heartfelt thanks for all the ooh-ing and ahh-ing done whenever I explained my research, your words of kindness, motivation, and advice, and always being ready for a game of Nertz when I needed a break. I couldn't have done it without you.

## ABSTRACT

Wildfires are an integral process in vegetative terrestrial land which shape ecosystem functions. A warming climate, however, has increased the size and severity of fires with significant ecosystem and societal implications. Furthermore, warming has changed characteristics of wildfires enabling a median upslope advance of 252 m in high-elevation forest fires from 1984 to 2017, allowing wildfires to burn in areas that were previously too wet to burn frequently. This exposed an additional 81,500 square kilometers (11%) of western US montane forests to fires.

In this thesis, I test the hypothesis that wildfires burn more intensely in high-elevation mesic forests than low-elevation dry forests. To this end, I assess fire intensity, which refers to how much heat energy is released during a fire, across the elevation gradient. I use satellite-observed fire radiative power (FRP) that measures the amount of radiant energy released from burning vegetation during a wildfire event as a proxy for fire intensity. FRP data are acquired from the MODIS sensor aboard Terra and Aqua satellites for fires between 2000 and 2021 which are then paired with elevation data using digital elevation maps. I derive this data for the 15 mountainous ecoregions of the western US and conduct various hypothesis tests to determine whether or not there is a statistically significant trend in FRP as a function of elevation. I will also assess whether or not the distribution of FRP for high-elevation and low-elevation wildfires are equal.

Among the 15 studied mountainous ecoregions, 12 ecoregions are associated with a statistically significant increasing FRP as a function of elevation, 1 is associated with

statistically non-significant increase in FRP as a function of elevation, and 2 were associated with statistically significant decreasing FRP as a function of elevation. I note the limitations of satellite-derived FRP, including twice-a-day overpass of satellite over fires, limitations of the MODIS sensor in capturing small fires, and algorithmic errors in inferring FRP from thermal anomaly observations. Nevertheless, long-term (20+ years) observation of FRP provides unparalleled opportunities for geospatial and temporal analysis of trends in fire intensity. Furthermore, quantile regression analysis revealed that higher intensity fires increase at a higher rate compared to lower intensity fires as a function of elevation. Finally, my analysis showed that 10 of the studied ecoregions are associated with statistically significant increase in FRP as a function of year (i.e., fires are intensifying in recent years), 1 has a statistically non-significant increasing trend, 2 ecoregions don't show any trend in FRP as a function of year, and 2 are associated with statistically non-significant trends in FRP versus year.

High-elevation wildfires and their intensity are important for societal and ecological systems that are affected by wildfires. They impact, for example, quantity and quality of water resources for 70% of the western US population that depend on high-elevation areas as their source of water. Understanding this phenomenon can inform wildfire and land management in a warming climate.

## TABLE OF CONTENTS

DEDICATION.....	iv
ACKNOWLEDGEMENTS.....	v
ABSTRACT .....	vi
LIST OF TABLES .....	x
LIST OF FIGURES .....	xi
LIST OF ABBREVIATIONS.....	xiii
CHAPTER 1: INTRODUCTION.....	1
CHAPTER 2: BACKGROUND.....	2
2.1 Global Fire Background.....	2
2.2 US Fire Drivers.....	4
2.3 US Forest and Fire Ecology .....	11
2.4 Fire Radiative Power .....	17
2.5 Western US Fire Background.....	18
CHAPTER 3: DATA COLLECTION .....	23
3.1 EPA Level III Ecoregions .....	23
3.2 MODIS Active Fire Data .....	24
3.3 US Geological Survey Digital Elevation Model .....	27
3.4 ArcGIS Pro Compilation.....	28
3.5 Discussion .....	30



CHAPTER 4: DATA ANALYSIS .....	31
4.1 Research Questions .....	31
4.2 Methods .....	31
4.3 Statistical Hypothesis Test Results .....	32
4.3.1 Student’s T-test.....	32
4.3.2 Augmented Dickey-Fuller Test .....	33
4.3.3 Fligner-Killeen Test.....	34
4.3.4 Remaining Tests .....	35
4.4 Graphical Analysis Results.....	39
4.4.1 Fire Radiative Power Trends Over Time .....	39
4.4.2 Fire Radiative Power Trends Over Elevation.....	43
4.5 Discussion.....	46
CHAPTER 5: SUMMARY.....	48
5.1 Summary.....	48
5.2 Future Research.....	51
REFERENCES.....	52

## LIST OF TABLES

Table 2.1	USDM drought categories (USDM 2022).....	8
Table 3.1	MODIS sensor band specifications.....	26
Table 3.2	FRP-elevation dataset for analysis.....	29
Table 4.1	Student’s T-test results.....	33
Table 4.2	Augmented Dickey-Fuller test results.....	34
Table 4.3	Fligner-Killeen test results .....	35
Table 4.4	Analysis results for the remaining 7 tests.....	38

## LIST OF FIGURES

Figure 2.1	Annual and seasonal precipitation changes in the western US from 1901 to 2015 (Easterling et al. 2017).....	5
Figure 2.2	Annual average temperatures in the western US from 1895 to 2020 (NOAA 2020).....	6
Figure 2.3	USDM archive map from August 25th, 2020 (USDM 2022).....	9
Figure 2.4	USDM archive map from August 24, 2021 (USDM 2022).....	10
Figure 2.5	Elevational distribution of vegetation (Remke et al. 2021).....	12
Figure 2.6	Low-elevation dry forest (Rush 2020).....	13
Figure 2.7	High-elevation mesic forest (Ziel 2020).....	14
Figure 2.8	Measures of fire severity (Berger et al. 2018) .....	16
Figure 2.9	Fire severity and intensity (United Nations Environment Programme 2022).....	17
Figure 2.10	Upslope advance of high-elevation wildfires in the western US (Alizadeh et al. 2021) .....	21
Figure 3.1	Mountainous ecoregions of the western US .....	24
Figure 3.2	Orbital paths of Terra and Aqua satellites (Levy et al. 2018).....	25
Figure 4.1	FRP values in each year.....	40
Figure 4.2	Trends in FRP values as a function of year .....	41
Figure 4.3	Quantile regression of the slope of FRP values over time.....	42
Figure 4.4	FRP values in each elevation group .....	43
Figure 4.5	Trends in FRP values versus elevation.....	45

Figure 4.6 Quantile regression of the slope of FRP values versus elevation..... 46

## LIST OF ABBREVIATIONS

ANOVA	Analysis of Variance
BLM	Bureau of Land Management
BSU	Boise State University
DEM	Digital Elevation Model
EPA	Environmental Protection Agency
FIRMS	Fire Information for Resource Management Systems
FRP	Fire Radiative Power
GIS	Geographic Information System
LANCE	Land, Atmosphere Near real-time Capability for EOS
MODIS	Moderate Resolution Imaging Spectroradiometer
NASA	National Aeronautics and Space Administration
NOAA	National Oceanic and Atmospheric Administration
NRT	Near Real-Time
US	United States
USDM	United States Drought Monitor
USGS	United States Geological Survey
VPD	Vapor Pressure Deficit



## CHAPTER 1: INTRODUCTION

Historically, wildfires have provided many integral services for ecosystems around the globe, however, fire exclusion efforts and changes in wildfire behavior due to a warming climate threatens this symbiotic relationship (Binkley et al. 2007). In recent decades, burn area, fire size and the occurrence of large fires has increased in many regions of the world, though an increase in the average elevational distribution of wildfires in montane environments of the western United States is of particular concern (Dennison et al. 2014; Westerling 2016). Recent studies present changing fire characteristics and an upslope advance of wildfires in many ecoregions across the western US. These high-elevation wildfires and their intensity can have a detrimental effect on terrestrial carbon storage, snowpack, and the quantity and quality of water resources, as well as air pollution, climate, food supply, and biodiversity (Alizadeh et al. 2021; Keeley 2009).

Although management policies and fire behavior models have greatly advanced since initial integration, few studies have been dedicated to studying the increase in elevational distribution of wildfires, and yet even fewer focused on studying the changing fire characteristics at these elevations. The purpose of this study is to analyze the relationship between fire intensity and elevation in mountainous regions of the western US, and to better understand the development of this wildfire characteristic to inform wildfire and land management in a changing climate.

## CHAPTER 2: BACKGROUND

Warmer temperatures over time are changing weather patterns and disrupting the usual balance of nature. Particularly in montane environments, there has been an increase in temperature with elevation gain, longer snow-free periods, increased evaporative demand, declines in precipitation during the fire season (especially in the western US), and even an increase in the number of convective storms and lightning strikes due to a warming climate (Abatzoglou and Williams 2016; Del Genio et al. 2007; Holden et al. 2018; Pepin et al. 2015; Westerling et al. 2006). These factors contribute to a change in wildfire activity by providing an excess of dry fuel during the typical fire season.

### **2.1 Global Fire Background**

Propelled by centuries of industrial and agricultural expansion and intensification, global warming and climate change have had immense effects on natural ecosystems. Global-mean surface temperature (GMST) is a significant indicator of global climate change, and is most directly related to climate impacts and threats. Despite natural climate variability, GMST accelerated since the 1970's (Rahmstorf et al. 2017) and displayed three record-hot years in 2016, 2019, 2020. These high temperatures have been a cause for severe concern with fire. As winter temperatures climb, spring snowmelt occurs earlier in the year which in turn intensifies dry conditions in the summer (Flannigan et al. 2009). As this water deficit increases, the abundance of dry fuel leads to an increase in wildfire activity in fire prone areas.



Regions across the world are seeing an increase in wildfire frequency and intensity as these devastating fires sweep through natural ecosystems and human-dominated landscapes. Mega-fires, or fires covering tens to hundreds of thousands of hectares, have become a common occurrence in fire regimes across the globe, particularly in the boreal forests of Northern Eurasia and North America (Natole et al. 2021; Khorshidi et al. 2020). In 2003, for example, Eastern Siberia experienced one of the largest fire years on record, burning over 22 million hectares over the course of the year (Talucci et al. 2022). The summer of 2010 saw more than 6 hundred wildfires break out in western Russia due to an immense heatwave (Guo et al. 2017). In the southern hemisphere, 2020 was an exceptionally devastating year for fire activity as well. The Australian bushfires destroyed over 24 million hectares and killed 34 people as well as an estimated 1 billion wild mammals, birds and reptiles (Lewis 2020).

Record-breaking wildfires are becoming increasingly common worldwide, and concern about the effects of climate change and humans on these events grow with it. Emissions produced by wildfires significantly impact global atmospheric composition, climate, and environmental pollution from extensive biomass consumption which contributes to atmospheric particulates and greenhouse gases in the troposphere (Crutzen and Andreae 1990; Garbaras et al. 2015). Global projections show that a temperature-driven fire regime will dominate the 21st century, showing that future climate factors will play a larger role than human drivers in fire trends (Pechony and Shindell 2010). Regardless of the factors that play a role in this trend, the fact remains that fire and climate scientists and engineers are left to prepare for an increasingly flammable world.

## 2.2 US Fire Drivers

Increasing trends in wildfire activity across the western US are enabled by many factors. Anthropogenic climate change, natural climate variability, and a history of human settlement and fire suppression activities have been conducive to an increase in fire frequency and intensity, as well as the area burned by these wildfires (Abatzoglou and Williams 2016; Baker 1993; Cooper 1960).

Climate primarily influences wildfire activity by supplying combustible fuel in environments that are primed for wildfire, and human-driven climate change is an important contributor to increased wildfire potential in the western US (Abatzoglou and Williams 2016). Changes in precipitation can have the most detrimental effect in a warming climate because a continuous water supply is essential to societies and ecosystems. Although these systems have developed over time to adapt to variations in precipitation, the rapidity of changing trends shows signs of harmful transformations in these systems. Between 1901 and 2015, average annual precipitation across the contiguous US increased approximately 4 percent, however, due to recent lingering droughts in the western and southwestern US, some trends have declined (Easterling et al. 2017). Figure 2.1 shows the apparent differences in annual precipitation for the regions of the US. Changes in precipitation differ throughout the year, as do regional patterns of increases and decreases. For the contiguous US, fall shows the largest national increases, while there is little observed change in the winter. When comparing regionally, the Northeast, Midwest, and Great Plains have had increases in precipitation while parts of the Southwest and Southeast have had decreases. Winter precipitation averages has the smallest increase (2%), with drying over most of the western United States in fire prone

areas. In spring, the northern half of the contiguous United States has become wetter, while the southern half has become drier. In summer, there is a mix of increases and decreases across the US.

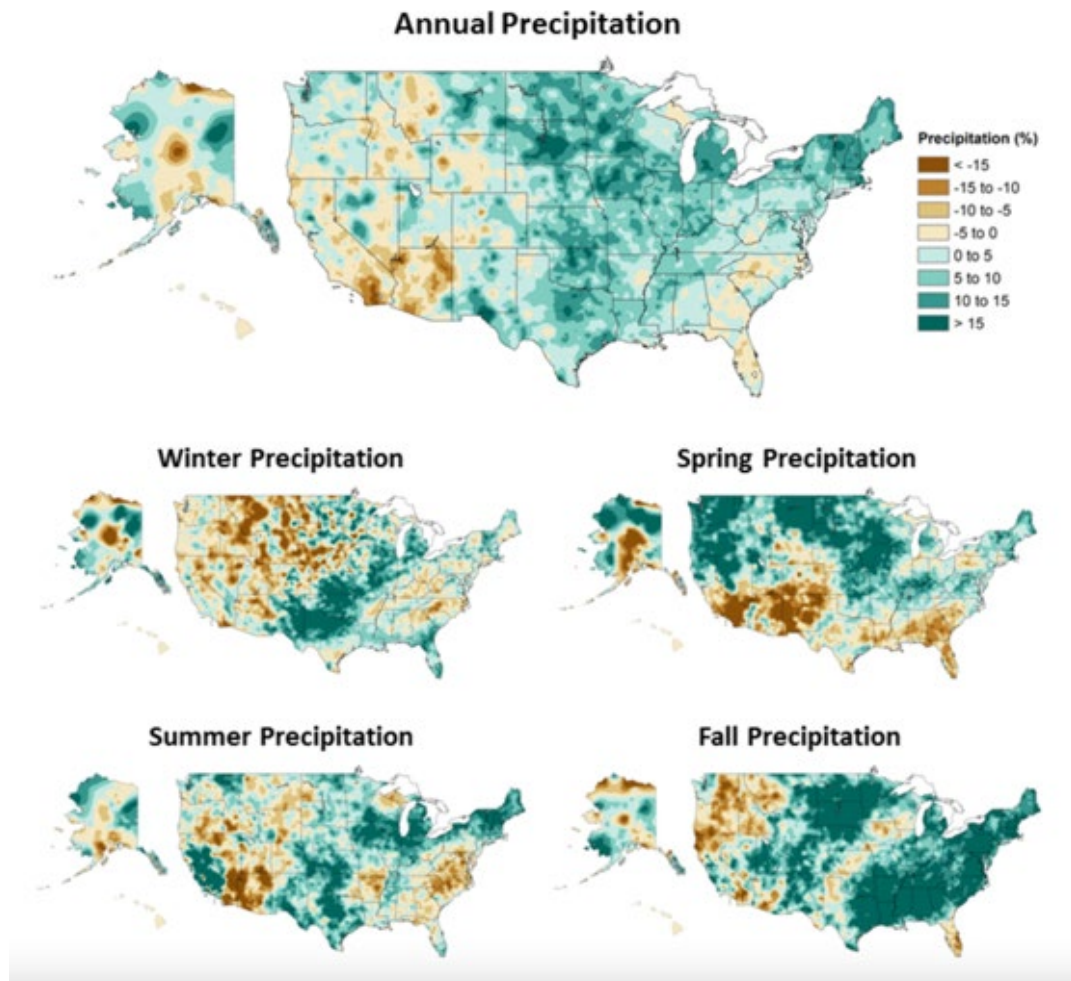


**Figure 2.1** Annual and seasonal precipitation changes in the western US from 1901 to 2015 (Easterling et al. 2017)

In much of the western US, forested areas are concentrated in mountain ranges where the elevation increases the chance of winter precipitation to be in the form of snow (Barry 1992). The snow can then accumulate and carry this moisture from the cool season into the more arid summer, providing a source of water for agriculture, the public, hydropower, and recreation throughout the year. However, since 1980, much of the

western US has seen declines of end-of-season snow water equivalent (SWE), particularly in areas that depend on spring snow melt as their main water supply (Easterling et al. 2017). The western US has become a hot-spot for snow droughts, with an increase in snow drought duration of 28% between 1980 and 2018 (Huning and AghaKouchak 2020). This shift in the timing of spring snowmelt and the decreased quantity of SWE in the snowpack can significantly influence the length of the fire season and the amount of combustible fuel (Westerling 2016).

Since the 1970's, human-driven increases in temperature have led to an abundance of combustible fuel across western US forests (Abatzoglou and Williams 2016). Figure 2.2 acquired from the National Oceanic and Atmospheric Administration (NOAA) shows annual average temperatures in the western US from 1895 to 2020. The solid black line represents the mean temperature between 1896 and 2020. With temperatures from 1995 forward frequently above the overall mean, it is clear there is an increasing trend in temperature in the western US.

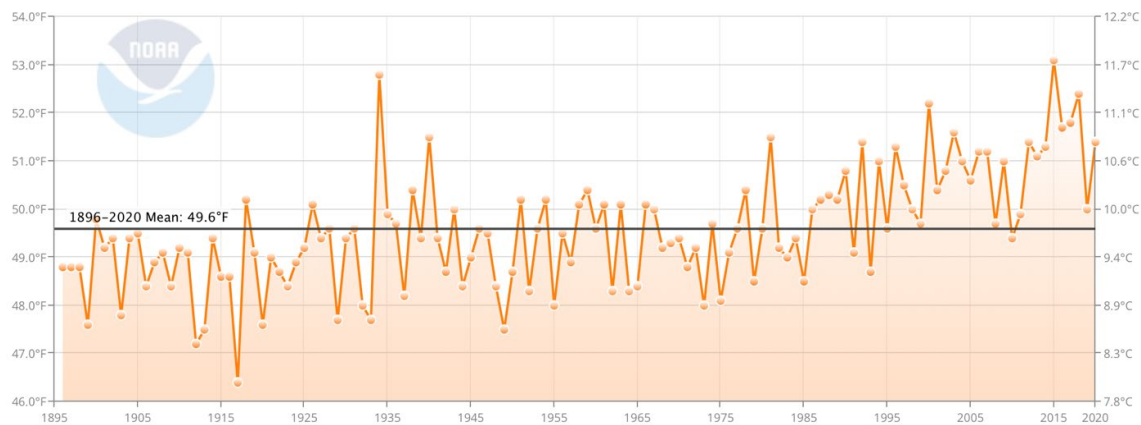


**Figure 2.2 Annual average temperatures in the western US from 1895 to 2020 (NOAA 2020)**

Warmer air can hold more moisture, so as temperatures rise, evaporation pulls more water from plants and soil, thus leading to drier conditions. Combined with declines in precipitation in the western US, and it creates a long-term drought.

Changes in the intensity and duration of droughts can dramatically affect ecosystems, agriculture, food and water security, hydropower, and wildfire activity. The United States Drought Monitor (USDM) is produced jointly by the National Drought Mitigation Center at the University of Nebraska-Lincoln, the National Oceanic and Atmospheric Administration (NOAA), and the US Department of Agriculture (USDA). The USDM is a map updated weekly showing the location and intensity of drought across the US. There are five classifications for drought across the US: Abnormally Dry (D0), showing areas that may be going into or are coming out of drought, as well as Moderate (D1), Severe (D2), Extreme (D3) and Exceptional (D4) Drought. These categories are determined by drought experts observing various conditions related to drought, such as how much available water there is in nearby streams, lakes, and soils compared with a typical observation for that time of year. These observations take into account precipitation totals, temperature, soil moisture, water levels, snowpack, and snowmelt runoff (United States Drought Monitor 2022). Table 2.1 denotes the five USDM drought categories with their corresponding possible impacts.

**Table 2.1** USDM drought categories (USDM 2022)

Category	Description	Possible Impacts
D0	Abnormally Dry	Going into drought: <ul style="list-style-type: none"> <li>• short-term dryness slowing planting, growth of crops or pastures</li> </ul> Coming out of drought: <ul style="list-style-type: none"> <li>• some lingering water deficits</li> <li>• pastures or crops not fully recovered</li> </ul>
D1	Moderate Drought	<ul style="list-style-type: none"> <li>• Some damage to crops, pastures</li> <li>• Streams, reservoirs, or wells low, some water shortages developing or imminent</li> <li>• Voluntary water-use restrictions requested</li> </ul>
D2	Severe Drought	<ul style="list-style-type: none"> <li>• Crop or pasture losses likely</li> <li>• Water shortages common</li> <li>• Water restrictions imposed</li> </ul>
D3	Extreme Drought	<ul style="list-style-type: none"> <li>• Major crop/pasture losses</li> <li>• Widespread water shortages or restrictions</li> </ul>
D4	Exceptional Drought	<ul style="list-style-type: none"> <li>• Exceptional and widespread crop/pasture losses</li> <li>• Shortages of water in reservoirs, streams, and wells creating water emergencies</li> </ul>

Figure 2.3 is a USDM archive map from August 25th, 2020. A majority of the western US is seen in the Severe Drought category with some Abnormally Dry, Moderate, and Extreme Drought areas scattered throughout. Areas in white mean there is no sign of drought in those locations.

*U.S. Drought Monitor*  
**Continental U.S. (CONUS)**

**August 25, 2020**  
*(Retrieved Thursday, Aug. 27, 2020)*  
Valid 8 a.m. EDT

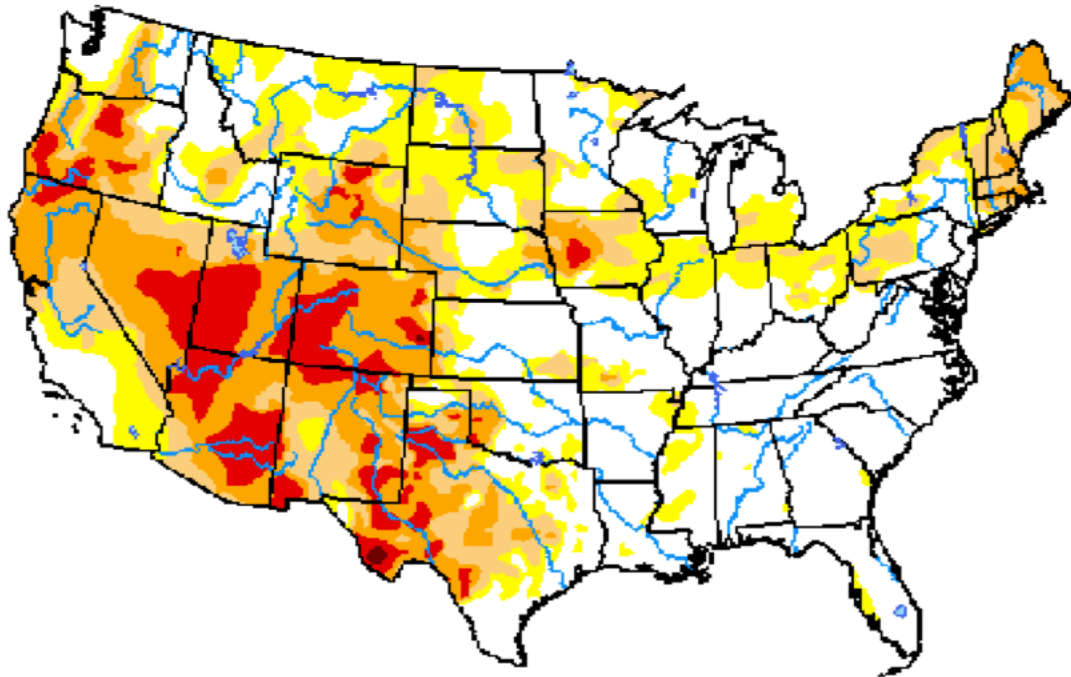


**Figure 2.3** USDM archive map from August 25th, 2020 (USDM 2022)

Figure 2.4 shows a USDM archive map from August 24th, 2021, one year after that of Figure 2.3. Areas in the West – in particular Montana, Idaho, Washington, Oregon, California and Nevada - that were previously at an Abnormally Dry level (Figure 2.3) now shifted towards Severe Drought and even Extreme and Exceptional Drought (Figure 2.4).

*U.S. Drought Monitor*  
**Contiguous U.S. (CONUS)**

**August 24, 2021**  
(Released Thursday, Aug. 26, 2021)  
Valid 8 a.m. EDT

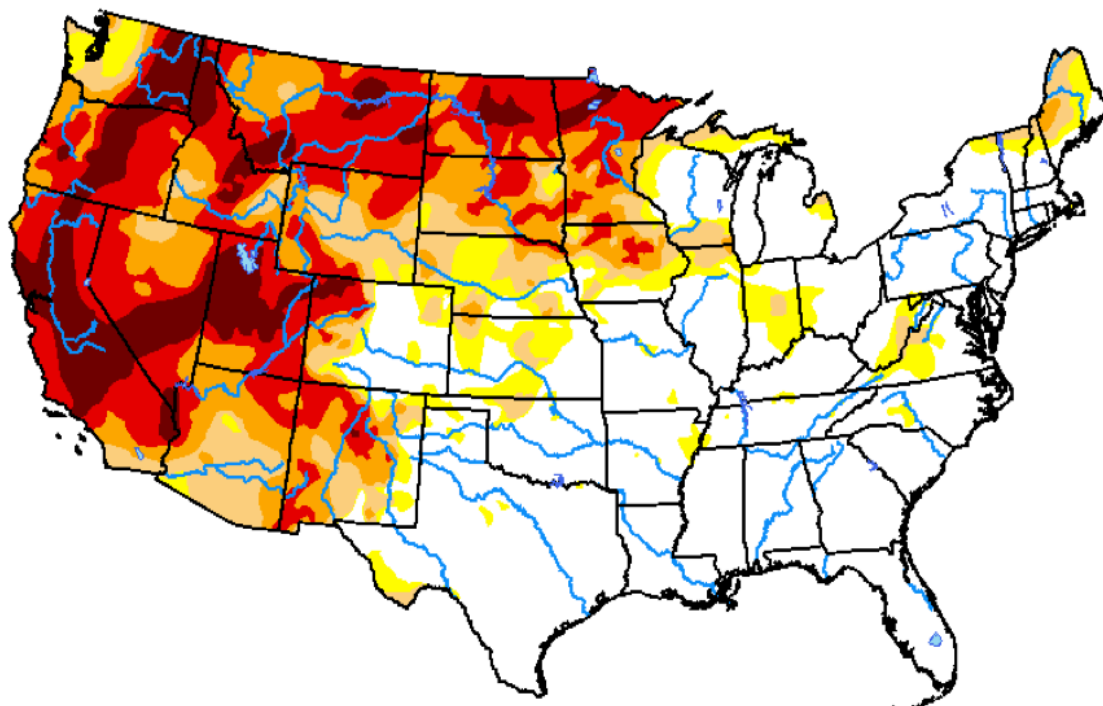


**Figure 2.4** USDAM archive map from August 24, 2021 (USDAM 2022)

When paired with declines in precipitation, an earlier spring snowmelt, warming temperatures, and more intense droughts across the western US, vegetation is more combustible during drought, which means these forests are now primed for wildfires.

The spark needed to ignite a wildfire can be either human or natural, and with more frequent convective storms and consequent lightning strikes due to a warming climate, it is not uncommon for wildfires to naturally begin (Del Genio et al. 2007). Lightning-caused wildfires primarily occur in the mountainous western US, and from 1992 to 2012, these ignitions only amounted to 0.7 million square kilometers compared to 5.1 million square kilometers for human-caused wildfires (Balch et al. 2017). Although



ongoing research tends to focus on increased risk of wildfire due to climate warming, people play a direct role in igniting wildfires and increases in wildfire activity.

Anthropogenic ignitions accounted for 84% of all wildfires and 44% of total area burned across the US from 1992-2017. Between 1992 and 2012, the human-caused fire season was three-times longer than the lightning-caused fire season and humans added 40 thousand wildfires per year (Balch et al. 2017).

Fire suppression activities and the reduction of logging since the late 19<sup>th</sup> century has changed the structure and growth of forests to potentially increase large-scale wildfires. Passage of the federal Clarke-McNary Act in 1924 created a national fire-suppression policy, promoting “better” forest protection, namely in fire control and water resource usage (Stephens and Ruth 2005). Decades later, significant changes in the structure, composition, and available fuel were documented in forests in the western US (Baker 1993; Cooper 1960). Forests that typically saw low to moderately intense wildfires are now experiencing high-severity wildfires partially attributed to fire suppression practices.

The combination of anthropogenic climate change, natural climate variability, and historical fire suppression activities has propelled wildfire activity in the western US. Among these factors, climate change played a particularly larger role in high-elevation montane environments, since historical fire suppression was minimal in the highlands.

### **2.3 US Forest and Fire Ecology**

Forests and grasslands provide a variety of ecosystem services. The US has 141 different types of forests, which fall under three different categories: Tropical forests, Temperate forests, and Boreal forests (Ruefenacht et al. 2008). In much of the western

US, there are low-elevation dry forests and high-elevation mesic forests falling within the Temperate and Boreal categories (Jain and Graham 2015). Figure 2.5 shows how vegetation changes with elevation gain. In the warm and dry climates of lower elevation forests, vegetation is sparser with branches higher off the ground, which inhibits canopy fire and wildfire growth due to the low connectivity between available fuel. At higher elevations, the vegetation is denser with branches closer to the ground, allowing wildfires to spread more easily through the connected vegetation.

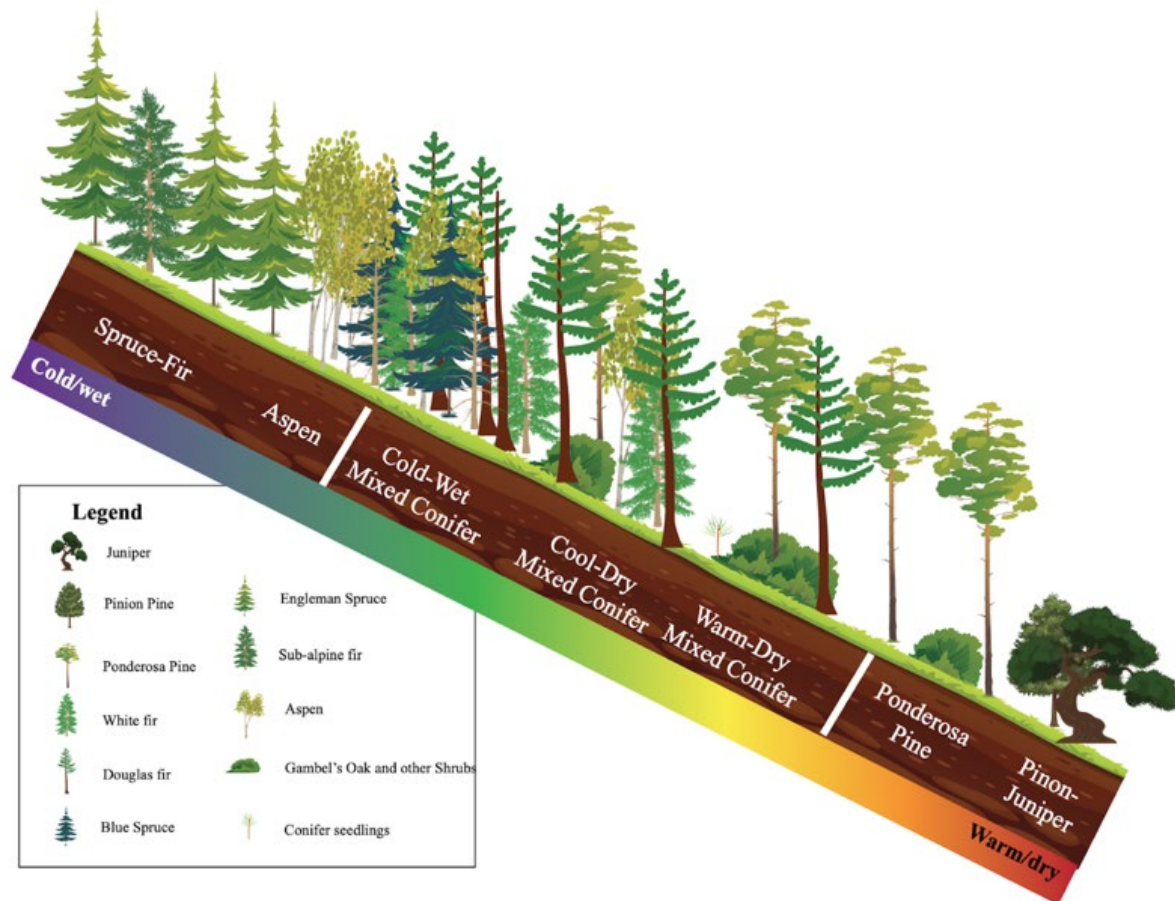


**Figure 2.5 Elevational distribution of vegetation (Remke et al. 2021)**

Figure 2.6 shows a low-elevation dry forest with only one of the surrounding trees burnt from wildfire. Although vegetation is dry and temperatures are warm in these

forests, without connectivity, wildfires have more difficulty spreading. The remaining juniper trees, sagebrush, and grasses remain undamaged despite the proximity to the wildfire.



**Figure 2.6 Low-elevation dry forest (Rush 2020)**

High-elevation mesic forests, however, are dense forests that typically have a moderate supply of moisture, but the changing climate of these areas has led to an abundance of combustible fuel. Once there is ignition, the trees and surrounding vegetation dry each other out and burn together, resulting in wildfires that are more intense and produce more energy, that results in stand-replacing impacts such as shown in Figure 2.7.





**Figure 2.7 High-elevation mesic forest (Ziel 2020)**

Differences in the diversity and distribution of these forests can have dramatically different results after a wildfire is done burning. Fire ecology looks into this issue more thoroughly.

Fire ecology is a scientific discipline that examines the dependence and adaptation of plants and animals to wildfires, and studies fire history and regime, and the effects of wildfire on ecosystems (Binkley et al. 2007). Wildfires play a key role in maintaining habitat heterogeneity, and there are many fire-dependent ecosystems around the world that rely on wildfires to maintain a healthy biodiversity (Herrando and Brotons 2002; Liu et al. 2010). However, due to a combination of factors including climate change, fire suppression policies, and other human-related activities, these fire-dependent forests in the US are seeing increasingly more intense wildfires (Dale 2006).

When it comes to inspecting the effects of a wildfire on ecosystems, fire ecologists will often use terms like severity and intensity. Fire severity, and the related term burn severity, refers to the quantitative measure of the effects of a wildfire on the environment in the burned area. It is measured in terms of tree mortality, canopy loss, crown scorch, and if there is evidence of a hydrophobic layer in the soil. Fire severity can be influenced by the amount of available fuel, the moisture content of the combustible material, the topography of the burn environment, as well as the weather conditions such as wind, temperature, and humidity (Berger et al. 2018). Figure 2.8 shows how severity can be broken down into 3 sub-categories: Unburned/low severity, Moderate severity and High severity.

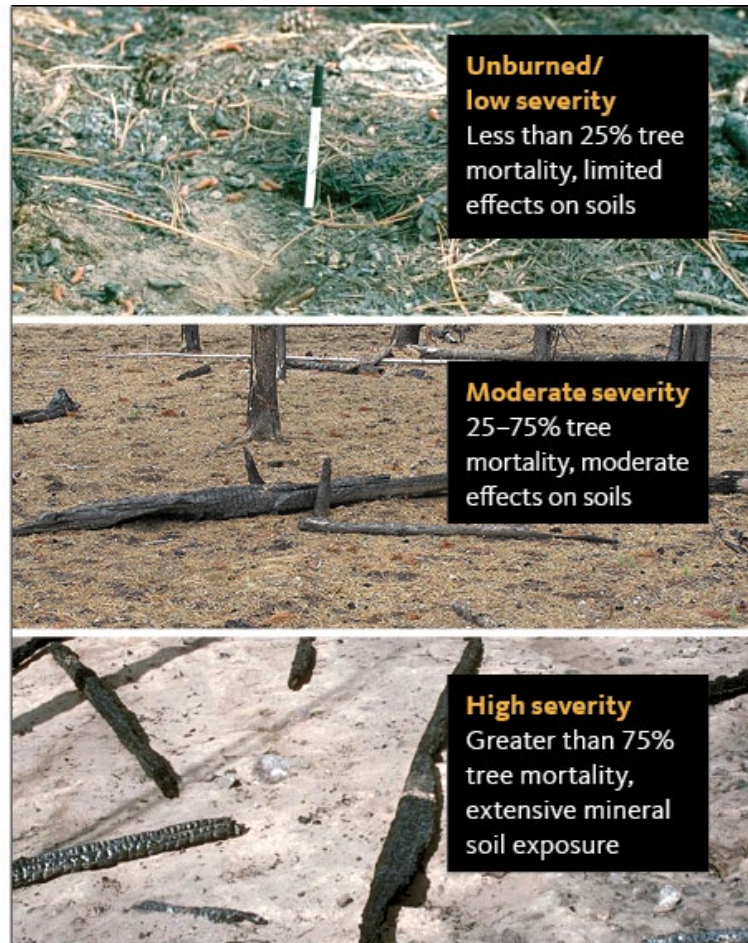


**Figure 2.8 Measures of fire severity (Berger et al. 2018)**

These classifications depend on tree mortality and how much the wildfire affected the soil in the burned area. It's assumed that these classifications are a good measure of vegetation post-fire regeneration ability, or a reflection of an ecosystems ability to recover after a wildfire event (Keeley 2009). As the amplitude and severity of a wildfire depends on how intensely a fire burns and the nature of the vegetation it is burning, these measures of fire severity are often correlated to measures of fire intensity. Figure 2.9 illustrates how fire severity and intensity are related. For a high-intensity fire, this will generally result in a high severity fire that has full crown defoliation, or complete tree mortality where no live vegetation remains. A moderately intense fire will see crown scorching in trees and charring in vegetation that is closer to the ground. Low-intensity

fires can have an unburned canopy with the lower vegetation being scorched or charred which signifies a less severe fire.

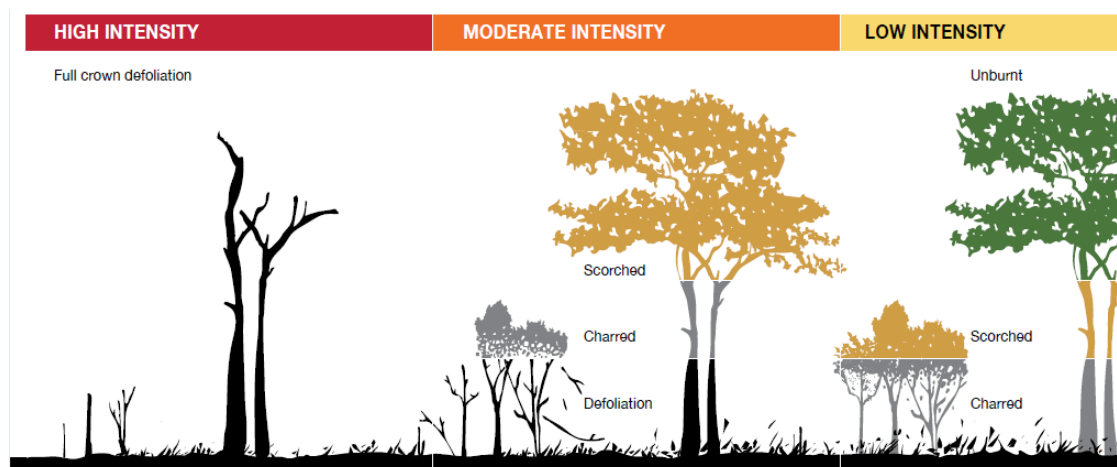


**Figure 2.9 Fire severity and intensity (United Nations Environment Programme 2022)**

Fire intensity refers to the rate of heat energy released during various phases of a fire. It can represent wildfires' reaction intensity, fire line intensity, temperature, heating duration, and radiant energy, though a widely used measurement of fire intensity is fire line intensity, which is the rate of heat transfer per unit length of the fire line (Keeley 2009). This wildfire characteristic impacts fuel consumption, how much damage is done to the vegetation, the chemical composition of fire emissions, and how the wildfire spreads across the landscape (Laurent et al. 2019).

#### **2.4 Fire Radiative Power**

Combustible fuel can come in many forms, such as dead leaf litter, live foliage, and woody materials, and each contain stores of energy. When a wildfire burns, the vegetation releases this energy in the form of radiant energy, and this data is acquired using remote-sensing methods. Fire radiative power (FRP) is a technique to quantify

burned biomass by measuring the amount of radiant energy emitted per time unit during combustion (Costa and Fonseca 2017).

The amount of biomass consumed (BC) can be quantified using Equation (1), where  $A$  is the measure of the burned area ( $m^2$ ),  $B$  is the amount of biomass inside the burned area ( $kg/m^2$ ), and  $\beta$  is the combustion efficiency, or the rate of fuel that actually burned (Seiler and Crutzen 1980).

$$BC = A \times B \times \beta \quad (1)$$

The amount of burned biomass is estimated using Equation (2), where BCR is the biomass consumption rate ( $kg/s$ ),  $C_e$  is the biomass consumption coefficient ( $kg/MJ$ ), and the FRP value obtained from satellite data (Wooster et al. 2005).

$$BCR = C_e \times FRP \quad (2)$$

The FRP value is quantified using remotely sensed data as the total fire intensity minus the energy dissipated from conduction and convection. It is expressed in units of power (megawatts), and is used to develop critical fire behavior models, predict the likelihood of fire propagation, make fire impact assessments, provide biomass combustion rates, predict emissions from fire, and advise fire management activities (Keeley 2009; Laurent et al. 2019). FRP is associated with fire intensity throughout the entire burning process, and is a method to quantify the intensity of wildfires (Barrett and Kasischke 2013; Wooster et al. 2005)

## 2.5 Western US Fire Background

Over the past several decades, the length of the fire season has increased similar to wildfire intensity, severity, and megafire frequency in the western United States. Since 1984, there has been an increasing trend in the occurrence of significant fires and total



burned area per year in the western US, particularly in mountainous regions (Baker 1993).

In November 2018, California's Camp Fire became the deadliest and most destructive fire in the state's history. In the first 24 hours of the wildfire's progression, the Camp Fire swept through the town of Paradise and other communities, resulting in 85 civilian fatalities and 3 firefighter injuries. Having destroyed more than 18,000 buildings, it also became the world's costliest disaster that year. The favorable conditions for the inferno involved 200 days of drought prior to the event which transformed the region's typically lush terrain into combustible fuel, as well as the wind gusts of up to 48 kilometers (30 miles) per hour (Griffin 2021).

The year of 2020 marked a time of unprecedented wildfire activity across the globe, but especially in the western US. The Cameron Peak Fire burned for nearly 4 months from August to December and became Colorado's largest wildfire on record. This mega-fire consumed 845 square kilometers (208,913 acres) and was spurred on by 129 kilometers (80 miles) per hour winds, all while the nearby East Troublesome Fire raised concerns for other reasons. The East Troublesome Fire began in October and soon became the second largest fire in Colorado's history by climbing to elevations around 2,743 meters (9,000 feet) and crossing the Continental Divide (National Park Service 2021).

In 2021, at the beginning of August, the Dixie and Caldor fires in northern California alarmed many by climbing to record elevations for the state above 2,438 meters (8,000 feet) and jumping the peaks of the Sierra Nevada Mountain range to the other side. The blaze became the state's third largest wildfire on record by consuming

1,752 square kilometers (432, 813 acres) amidst high temperatures and strong winds. The elevations at which the Caldor, Dixie, Cameron Peak, and East Troublesome fires burned at is unprecedented wildfire behavior, and a cause for severe concern.

There are many studies that show high-elevation forests that were once considered areas too wet to burn frequently are now at risk of wildfires, which strongly correlates with a warming climate. In the past, there are typically century- to millenia-long return intervals between fires in these wetter forests, or mesic forests, at high elevations. Now they are experiencing the highest rate of increase in fire activity seen in the last 34 years (Sadegh et al. 2021).

A recent study spanning from 1984 to 2017 documented that wildfire occurrences and associated warm season vapor pressure deficit (VPD) have shifted towards higher elevations in the western US (Alizadeh et al. 2021). This research was conducted for fifteen mountainous ecoregions in the western US, which documented a median upslope advance of 252 meters in high-elevation mesic forest fires between 1984 and 2017. Figure 2.5 presents the changes in in the 90th percentile of annual elevational distribution of wildfires for each ecoregion between 1984 and 2017. The dotted areas are associated with ecoregions that have statistically significant monotonic trends at the 5% level using the Mann–Kendall trend test. The hatched areas represent ecoregions with at least 10% length of record (4 years) excluded from the analysis due to absence of fire. The gray shaded ecoregions were not included in the study.

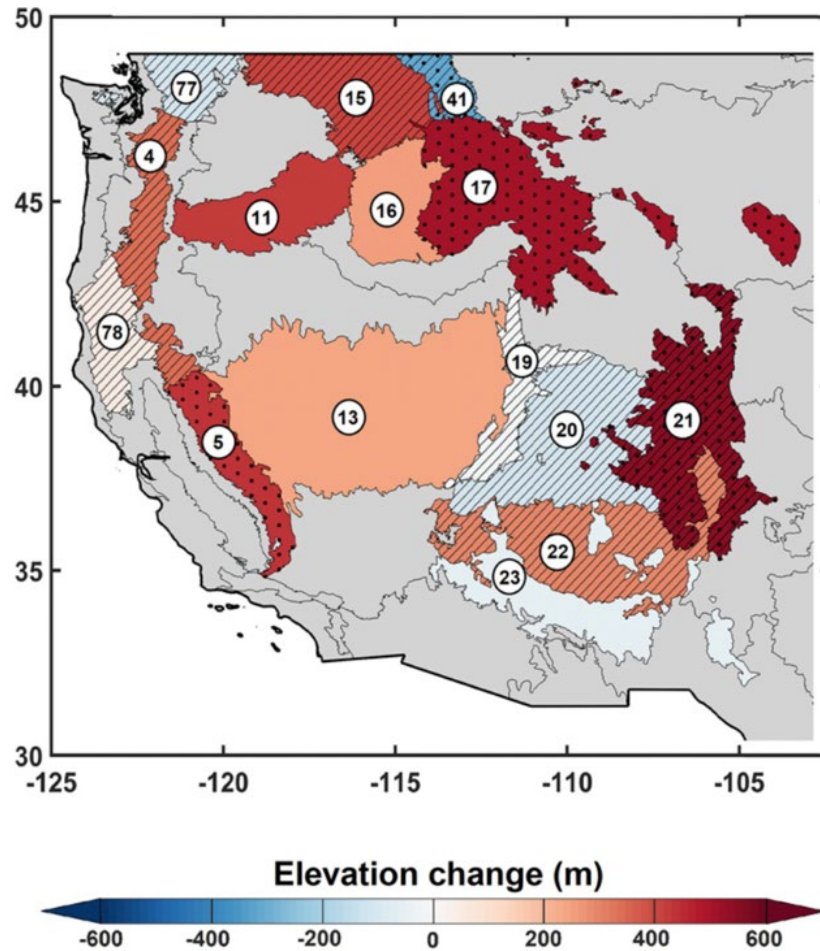


**Figure 2.10 Upslope advance of high-elevation wildfires in the western US (Alizadeh et al. 2021)**

Additionally, there was found to be a median upslope drift of warm season VPD of 295 meters over the time period, as well as evidence that the high-elevation flammability barrier has decreased. The combination of these factors allows wildfires access to 11% more area in western US forests in the past 34 years, exposing an additional 81,500 square kilometers of montane forests that previously went unburnt. This creates the potential to transform montane fire environments and detrimentally affect ecosystems and watersheds. An increase in wildfire activity at these elevations can dramatically affect terrestrial carbon storage, snowpack, and water quantity and quality in

the West (Alizadeh et al. 2021), but with so much untouched forest now bared to wildfires, there is the likelihood that these forest fires are significantly more intense as well.

Here I test the hypothesis that mesic forests burn at a higher intensity than dry forests across the elevation gradient. Though seemingly straightforward, this relationship may be complex and dependent on other factors such as topography, climate, fuel availability, density and connectivity, as well as fire management practices. The data collection, analysis, and discussion of this hypothesis can be found in Chapter 3 and Chapter 4.

## CHAPTER 3: DATA COLLECTION

In order to examine the energy released from wildfires across the elevation gradient, data was compiled to analyze the trends in high-elevation forest fires with respect to FRP. Data was acquired from multiple sources for the fifteen mountainous ecoregions of the western US, and geospatial data analysis was performed to construct a FRP and elevation dataset based on fires between 2000 and 2021 for each ecoregion. Specific details on how the data was collected can be found in this chapter.

### **3.1 EPA Level III Ecoregions**

The US Environmental Protection Agency (EPA) has identified areas where ecosystems are similar in terms of biotic, abiotic, terrestrial, and aquatic components and created ecoregions to serve as a spatial framework for research, assessment, and monitoring of these ecosystems (McMahon et al. 2001; Omernik 1987). There are four hierarchical levels of ecoregions, ranging from general regions in Level I to more detailed regions in Level IV (EPA 2022). This research adopted Level III Ecoregions containing 105 different ecoregions for the continental US, and then identified 15 mountainous ecoregions of the western US as shown in Figure 3.1. The ecoregions names are as follows: 4: Cascades, 5: Sierra Nevada, 11: Blue Mountains, 13: Central Basin and Range, 15: Northern Rockies, 16: Idaho Batholith, 17: Middle Rockies, 19: Wasatch and Unita Mountains, 20: Colorado Plateaus, 21: Southern Rockies, 22: Arizona/New Mexico Plateau, 23: Arizona/ New Mexico Mountains, 41: Canadian Rockies, 77: North Cascades, and 78: Klamath Mountains/California High North Coast Range.

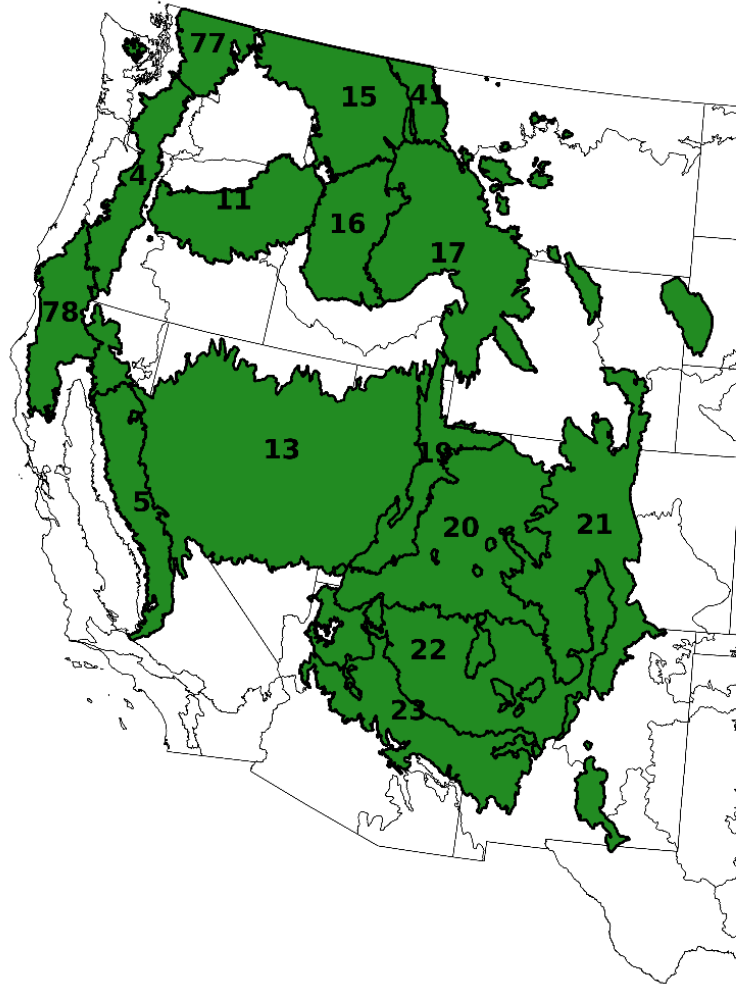


**Figure 3.1 Mountainous ecoregions of the western US**

Shapefiles were downloaded for each ecoregion, which were used to ensure the supplementary data used in analysis only existed within the perimeter of each ecoregion.

### **3.2 MODIS Active Fire Data**

Since it is not possible to go within an active fire perimeter to gather data, remote sensing is the most practical method for measuring the amount of energy released from wildfires. The Moderate Resolution Imaging Spectroradiometer (MODIS) instrument aboard the Terra and Aqua satellites has acquired fire data globally since 2000 at ground sampling intervals, or pixels, at approximately 1 kilometer resolution. Figure 3.2

demonstrates the satellites' orbital paths. The Terra satellite orbits north to south across the equator, and the Aqua satellite orbits south to North across the equator, crossing paths in order to view the earth's entire surface every 1 to 2 days (Giglio 2000).

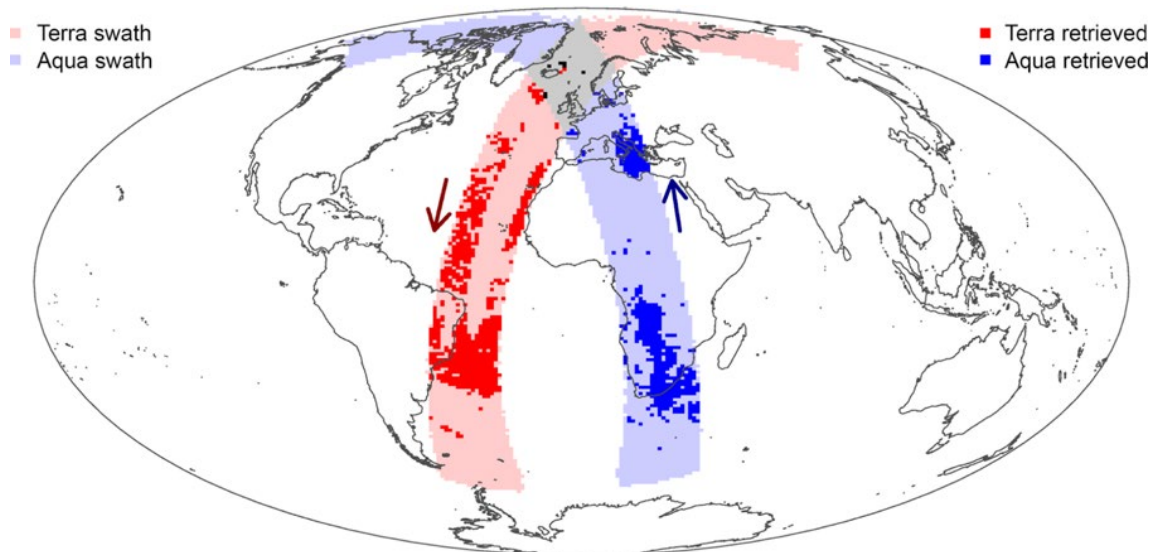


**Figure 3.2** Orbital paths of Terra and Aqua satellites (Levy et al. 2018)

The MODIS sensor measures electromagnetic radiation at 36 specific ranges, typically called bands or groups of wavelengths. The main ranges for non-contact temperature measurement the MODIS instrument processes are the visible region (405 to 753 nm), near infrared (NIR; 841 to 1390 nm), short-wave infrared (SWIR, 1628 to 2155 nm), and long-wave thermal infrared (TIR; 3.660 to 14.385  $\mu\text{m}$ ). The resulting pixels can be acquired at three spatial resolutions: 250, 500, and 1,000 meters (Giglio 2000). Table 3.1 shows the primary use, wavelength, spectral radiance, and spatial resolution for each band. The first seven bands provide an estimate for the surface spectral reflectance used to distinguish between land, clouds, and aerosols. The remaining bands at the 1,000-meter resolution measures the radiance, which corresponds to the brightness directed toward the sensor.

**Table 3.1 MODIS sensor band specifications**

Primary Use	Band	Wavelength	Spectral Radiance	Resolution
Land/Cloud/ Aerosols Boundaries	1	620 – 670 nm	21.8	250 m
	2	841 – 876 nm	24.7	250 m
Land/Cloud/Aerosols Properties	3	459 – 479 nm	35.3	500 m
	4	545 – 565 nm	29	500 m
	5	1230 – 1250 nm	5.4	500 m
	6	1628 – 1652 nm	7.3	500 m
	7	2105 – 2155 nm	1	500 m
Ocean Color/Phytoplankton/ Biogeochemistry	8	405 – 420 nm	44.9	1000 m
	9	438 – 448 nm	41.9	1000 m
	10	483 – 493 nm	32.1	1000 m
	11	526 – 536 nm	27.9	1000 m
	12	546 – 556 nm	21	1000 m
	13	662 – 672 nm	9.5	1000 m
	14	673 – 683 nm	8.7	1000 m
	15	743 – 753 nm	10.2	1000 m
Atmospheric Water Vapors	16	862 – 877 nm	6.2	1000 m
	17	890 – 920 nm	10	1000 m
	18	931 – 941 nm	3.6	1000 m
Surface/Cloud Temperature	19	915 – 965 nm	15	1000 m
	20	3.660 – 3.840 $\mu\text{m}$	0.43(300K)	1000 m
	21	3.929 – 3.989 $\mu\text{m}$	2.38(335K)	1000 m
	22	3.929 – 3.989 $\mu\text{m}$	0.67(300K)	1000 m
Atmospheric Temperature	23	4.020 – 4.080 $\mu\text{m}$	0.79(300K)	1000 m
	24	4.433 – 4.498 $\mu\text{m}$	0.17(250K)	1000 m
Cirrus Clouds Water Vapor	25	4.482 – 4.549 $\mu\text{m}$	0.59(275K)	1000 m
	26	1.360 – 1.390 $\mu\text{m}$	6	1000 m
	27	6.535 – 6.895 $\mu\text{m}$	1.16(240K)	1000 m
Cloud Properties	28	7.175 – 7.475 $\mu\text{m}$	2.18(250K)	1000 m
	29	8.400 – 8.700 $\mu\text{m}$	9.58(300K)	1000 m
Ozone	30	9.580 – 9.880 $\mu\text{m}$	3.69(250K)	1000 m
Surface/Cloud Temperature	31	10.780 – 11.280 $\mu\text{m}$	9.55(300K)	1000 m
	32	11.770 – 12.270 $\mu\text{m}$	8.94(300K)	1000 m
Cloud Top Altitude	33	13.185 – 13.485 $\mu\text{m}$	4.52(260K)	1000 m
	34	13.485 – 13.785 $\mu\text{m}$	3.76(250K)	1000 m
	35	13.785 – 14.085 $\mu\text{m}$	3.11(240K)	1000 m
	36	14.085 – 14.385 $\mu\text{m}$	2.08(220K)	1000 m



These measures are quantized and converted into 1 kilometer active fire pixels where each pixel, representing FRP, has a discrete value. Thermal anomalies, or active fires, represent the center of one of these pixels that has been determined by the MODIS MOD14/MYD14 Fire and Thermal Anomalies algorithm to contain one or more fires within the pixel (Giglio et al. 2003). Active fire data is readily available for download through NASA's Land, Atmosphere Near real-time Capability for EOS (LANCE) Fire Information for Resource Management System (FIRMS), which is the most basic product for identifying active fires and other thermal anomalies. Since FRP can be used as a proxy for fire intensity (Wooster et al. 2005), this data was used to test the hypothesis that mesic forests burn more intensely than dry forests.

Once FRP data was obtained for each ecoregion, geospatial data analysis was performed to merge the FRP values with their corresponding elevations and forested cover data into one dataset for analysis.

### **3.3 US Geological Survey Digital Elevation Model**

A digital elevation model (DEM) represents a bare-earth topographic surface excluding trees, buildings, and any other surface objects. The National Map 3D Elevation Program provides elevational information for mapping applications and research by creating DEMs from topographic maps and high-resolution light detection and ranging (LIDAR) data (USGS 2022).

LIDAR is a remote sensing method that uses a pulsed laser beam to measure distances to the ground via aircraft, although this data includes buildings, vegetation, and the ground. This data can then strip away the surface features to create the bare-earth

DEM at 1/3 arc-second resolution, or approximately 10-meter resolution (Ferguson et al. 2020).

Through the USGS National Geospatial Program and the National Map, DEMs and other geospatial data are public domain and can be freely downloaded. These DEMs were used as a vital component of the FRP-elevation dataset used in analysis.

### **3.4 ArcGIS Pro Compilation**

ArcGIS Pro is a desktop geographic information system (GIS) software that uses geoprocessing tools to build analytical models and apply spatial statistics to data (ArcGIS Pro 2022). This software was used to compile the various forms of data collected, then perform geospatial data analysis to construct a FRP and elevation dataset based on fires between 2000 and 2021 for each ecoregion.

Once compiled, each dataset consisted of a list of individual active fire pixels with the corresponding geographic coordinates, acquisition date and time of burn, what satellite captured the data, the FRP value in megawatts, whether the acquisition occurred during the day or at night, and the average elevation of the FRP pixel. The resulting dataset was then exported as a CSV file to be uploaded to Python where specific data was extracted for efficient analysis. The new dataset consisted of the acquisition date which also provided the year and month of the fire point, the FRP value, the elevation, day or night capture information, and what elevation group the pixel fell within. An example of this data can be seen in Table 3.2.

**Table 3.2 FRP-elevation dataset for analysis**

	ACQ_DATE	Year	Month	FRP	Elevation	DAYNIGHT	Elev_group
<b>0</b>	2008-06-30	2008	6	64.7	1855.803	D	1500-2000
<b>1</b>	2008-06-30	2008	6	174.7	2069.565	D	2000-2500
<b>2</b>	2013-08-19	2013	8	24.3	1799.275	N	1500-2000
<b>3</b>	2012-11-27	2012	11	11.8	1924.051	D	1500-2000
<b>4</b>	2014-06-15	2014	6	75.5	1996.909	D	1500-2000
<b>5</b>	2003-11-05	2003	11	15.4	2222.631	D	2000-2500
<b>6</b>	2004-11-14	2004	11	31.1	1786.837	D	1500-2000
<b>7</b>	2014-12-09	2014	12	6.3	2028.989	D	2000-2500
<b>8</b>	2016-08-19	2016	8	174.2	2378.933	N	2000-2500
<b>9</b>	2016-08-19	2016	8	973.3	2312.285	N	2000-2500
<b>10</b>	2016-08-19	2016	8	180.0	1993.990	N	1500-2000
<b>11</b>	2016-08-19	2016	8	2232.7	2021.914	D	2000-2500
<b>12</b>	2016-08-19	2016	8	2235.7	1952.718	D	1500-2000
<b>13</b>	2016-08-19	2016	8	171.4	1937.228	D	1500-2000
<b>14</b>	2016-08-19	2016	8	2235.6	1792.034	D	1500-2000
<b>15</b>	2016-08-19	2016	8	267.9	2037.617	D	2000-2500

### 3.5 Discussion

Although using satellite data is an effective and efficient way to collect and distribute data, there are also some concerns to address. An issue with MODIS active fire data collection is that the satellites only orbit the earth every 1 to 2 days, thus leaving time for wildfires to reach peak intensity levels outside of the viewing window. This can result in lower measured FRP levels than actual FRP values, as well as reporting lower FRP values from any smoldering that may have continued after the active fire was done burning. This element of satellite data collection has the potential to skew data, but due to the 21-year time frame and the enormity of the sample sizes used in this research, it can be assumed that there is enough data to overlook this issue.

By compiling the various forms of data in ArcGIS Pro into one dataset, analysis became an efficient process performed for each ecoregion. Chapter 4 describes the analysis of these datasets for the fifteen ecoregions of the western US.

## CHAPTER 4: DATA ANALYSIS

In order to analyze the compiled data and investigate the hypothesis that mesic forests burn at a higher intensity than dry forests, various tests were performed for each ecoregion to assess the relationship between FRP and elevation, and an assortment of graphs were plotted to best represent the trends in the data. All tests are available in the open source coding language Python, where a variety of graphs were also produced to be displayed in this chapter.

### 4.1 Research Questions

The focus of this thesis was to research the relationship between FRP and elevation in the western US. Two research questions were developed prior to analyzing the collected data. The questions were:

1. Do mesic high-elevation forests burn at a higher intensity than low-elevation dry forests? If so, does it hold for all mountainous ecoregions of western US?
2. Do fires burn more intensely in recent years compared to the 2000s?

### 4.2 Methods

Answering these research questions involved performing ten statistical hypothesis tests and various forms of graphical analysis. The statistical tests provided a quantitative analysis of trends, mean, variance, or distribution for each ecoregion. The various tests performed are as follows: the Student's T-test, the Augmented Dickey-Fuller test, the

Fligner-Killeen test, Analysis of Variance, the Kruskal-Wallis H test, Bartlett's test, the Shapiro-Wilk test, the D'Agostino-Pearson  $K^2$  test, the Mann-Whitney U test, and the Wilcoxon Signed-Rank test. The null and alternative hypotheses are described for each test, and the results are presented subsequently.

Graphical analysis is helpful in digesting large volumes of information in an efficient and coherent manner, and compiling the analyzed data together allows easy comparison between ecoregions. Figures are displayed for FRP trends over time and FRP trends over elevation for each ecoregion in section 4.4 Graphical Analysis.

### **4.3 Statistical Hypothesis Test Results**

#### **4.3.1 Student's T-test**

The Student's T-test is used to test the means of two or more samples drawn from a normally distributed population where the standard deviation is unknown. The null hypothesis states that there is no difference between the hypothesized means and the observed sample means, and that any measured difference is only due to chance. The alternative hypothesis is that there is, in fact, a difference in means (Yazici 2007).

This test was performed for all active fire data between 2000 and 2021 for the fifteen ecoregions, and each dataset was split in two with respect to the median elevation so the test could compare the FRP values of the low-elevation half and the high-elevation half. The p-value accepts the null hypothesis with a value greater than 0.05, but if the value is less than or equal to 0.05, it is rejected and the alternative hypothesis is accepted.

Table 4.1 shows the results.

**Table 4.1 Student's T-test results**

<b>Ecoregions</b>	<b>P-Value</b>
4	5.35E-52
5	4.93E-18
11	6.26E-17
13	1.57E-87
15	6.12E-09
16	2.98E-67
17	8.60E-50
19	0.2798
20	3.84E-16
21	4.92E-16
22	5.81E-10
23	0.0171
41	2.23E-05
77	2.49E-38
78	9.99E-08

The results display that Ecoregion 19 (Wasatch and Unita Mountains) was the only ecoregion to accept the null hypothesis for all fire records within the 21-year period. In conclusion, there is enough evidence to show that mean FRP values are different between high-elevation and low-elevation fires for a majority of the ecoregions at the 0.05 significance level. Further analysis shows that mean FRP is greater in the high-elevation half of the fire records compared to the low-elevation half.

#### 4.3.2 Augmented Dickey-Fuller Test

The Augmented Dickey-Fuller test is used on larger and more complicated time series data. It is used to determine if a time series is not stationary by having a unit root, or in this case, no existing trend in the data. A Unit Root test is the proper method for testing the stationarity of a time series, and this test is one of the most common forms,

with the alternative hypothesis implying the data is stationary. A stationary time series does not depend on the time at which the data was observed (Dickey and Fuller 1979; Fuller 1976). This test was performed for all active fire data for the time period, and Table 4.2 presents the results.

**Table 4.2 Augmented Dickey-Fuller test results**

<b>Ecoregions</b>	<b>P-Value</b>
4	0
5	0
11	2.12E-30
13	0
15	0
16	0
17	0
19	2.48E-30
20	0
21	0
22	4.10E-15
23	0
41	1.51E-28
77	3.46E-30
78	0

Since all ecoregions have respective p-values below the significance level of 0.05, there is sufficient evidence to say that a trend exists for FRP data with respect to elevation.

#### 4.3.3 Fligner-Killeen Test

The Fligner-Killeen test is a non-parametric test to determine the homogeneity of variances between populations based on ranks. The null hypothesis states that all populations have the same variance. To be performed, the test centers the data around the



median elevation, and the absolute values of the residuals, or errors, are calculated, which are then ranked. This test is useful for when the data is non-normal or has outliers (Conover et al. 1981). This test was performed for all active fire data for the time period, and Table 4.3 displays the results.

**Table 4.3 Fligner-Killeen test results**

<b>Ecoregions</b>	<b>P-Value</b>
4	0
5	1.35E-22
11	4.34E-18
13	2.31E-222
15	4.69E-14
16	0
17	5.65E-224
19	1.49E-05
20	1.14E-55
21	9.47E-73
22	3.11E-45
23	8.13E-06
41	1.20E-26
77	8.65E-110
78	1.71E-58

Based on the results, it can be determined that the ecoregions in this study have significantly different sample variances for the median-centered fire data.

#### 4.3.4 Remaining Tests

The seven remaining tests have been gathered below for brevity, since they confirm the already presented information. Each test is explained, and all results have been compiled in Table 4.4.

The Analysis of Variance (ANOVA) test allows a comparison between two or more groups to determine if the means of samples are the same (null hypothesis), or the alternative hypothesis that the population means are statistically different from each other. This test assumes the samples are independent and normally distributed, and that the population standard deviations of each sample set are equal, or homoscedastic (Hartmann et al. 2018). This test was performed by splitting each ecoregion's data around the median elevation to see if there were deviations in the FRP means of the two data halves.

The Kruskal-Wallis H test is the non-parametric alternative to the one-way ANOVA test. The test determines if the medians of two samples are different, with the null hypothesis that the medians are equal, and the assumption that the independent data has the same shape distributions (MacFarland and Yates 2016). This test is useful in determining if there is a significant difference between these two samples, so each dataset was split around the median elevation in order to perform this test on median FRP values in each half.

Bartlett's test is used to determine the homogeneity of variance in different populations. This test assumes normality, and that the variances of these populations are equal, where the alternative hypothesis rejects this assumption (Arsham and Miodrag 2011). This test was also performed by centering the data groups around the median elevation for all active fire data.

The Shapiro-Wilk test is a statistical procedure that determines if the data was drawn from a normal distribution. Determining the distribution of the data is important to confirm because natural, continuous data typically displays a bell-shaped curve (Shapiro

and Wilk 1965). If the null hypothesis is accepted, this means the data is symmetric about the mean, showing that data near the mean are more likely to occur than data far from the mean. This test was performed for all active fire data for the time period.

The D'Agostino-Pearson  $K^2$  test is a goodness-of-fit test of normality. This test assumes the random data is normally distributed with the exact same mean and variance, and is very useful in detecting non-normality (D'Agostino et al. 1990). This test was performed for all active fire data as well.

The Mann-Whitney U test is a non-parametric test of the null hypothesis that declares two independent populations have equal distributions. The alternative hypothesis states that one distribution is stochastically greater than the other (Corder and Foreman 2014). This test is also performed by splitting the data into two for all active fire data around median elevation.

The Wilcoxon Signed-Rank test is similar to the Mann-Whitney U test in that it is also a nonparametric test, however, it is used on two dependent samples to determine if their distributions are equal or not (Corder and Foreman 2014).

The results for these seven tests can be seen in Table 4.4 below presenting the p-value to accept or reject the null hypothesis for each test in the fifteen specified ecoregions. The column number corresponds to the following test:

1. ANOVA
2. The Kruskal-Wallis H test
3. Bartlett's test
4. The Shapiro-Wilk test
5. The D'Agostino-Pearson  $K^2$  test

6. The Mann-Whitney U test
7. The Wilcoxon Signed-Rank test

**Table 4.4 Analysis results for the remaining 7 tests**

Ecoregions	P-Value						
	1	2	3	4	5	6	7
4	5.35E-52	9.99E-08	0	0	0	1.11E-303	3.76E-219
5	4.93E-18	0.0046	0	0	0	0.0023	4.81E-08
11	6.26E-17	3.14E-12	0	0	0	1.57E-12	3.51E-10
13	1.57E-87	2.51E-146	0	0	0	1.26E-146	2.46E-124
15	6.12E-09	6.59E-07	2.69E-110	0	0	3.30E-07	2.10E-07
16	2.98E-67	2.40E-262	2.67E-304	0	0	1.20E-262	7.46E-244
17	8.60E-50	8.56E-102	0	0	0	4.28E-102	1.11E-107
19	0.2800	0.0213	2.77E-08	0	0	0.0106	0.0249
20	3.84E-16	7.14E-52	0	0	0	3.57E-52	7.13E-35
21	4.92E-16	5.46E-33	8.38E-75	0	0	2.73E-33	1.93E-32
22	5.81E-10	5.36E-15	2.76E-105	0	0	2.68E-15	2.29E-21
23	0.0171	3.35E-10	6.10E-41	0	0	1.68E-10	0.0445
41	2.23E-05	5.31E-17	3.69E-29	0	0	2.66E-17	8.85E-15
77	2.49E-38	3.32E-39	0	0	0	1.66E-39	2.37E-49
78	9.99E-08	1.57E-68	6.43E-10	0	0	7.86E-69	3.78E-47

Upon examination of the statistical analysis results from all ten tests, the only tests that returned an accepted null hypothesis was the Student's T-test and ANOVA (1) for Ecoregion 19. With the majority of the results accepting the alternative hypothesis, it can be determined that the FRP values in the high-elevation and low-elevation ranges in this study have statistically different means, sample variances, and distributions. Trends in the data are also evident due to the results from the Augmented Dickey-Fuller test, however, it is not clear if this is an increasing or decreasing trend. Therefore, graphical

analysis was also performed in order to visually test the hypothesis that fires in higher elevations burn more intensely than low-elevation fires in these fifteen ecoregions.

## **4.4 Graphical Analysis Results**

### **4.4.1 Fire Radiative Power Trends Over Time**

Visualization methods that display data over a time period are useful to identify trends and variations over time. In order to do so, the data was extracted using Python to plot histograms of FRP values per year over the time period. These histograms are a common graph to display frequency distributions, and they clearly display the shape, center and spread of the data. Figure 4.1 shows this data for each ecoregion.

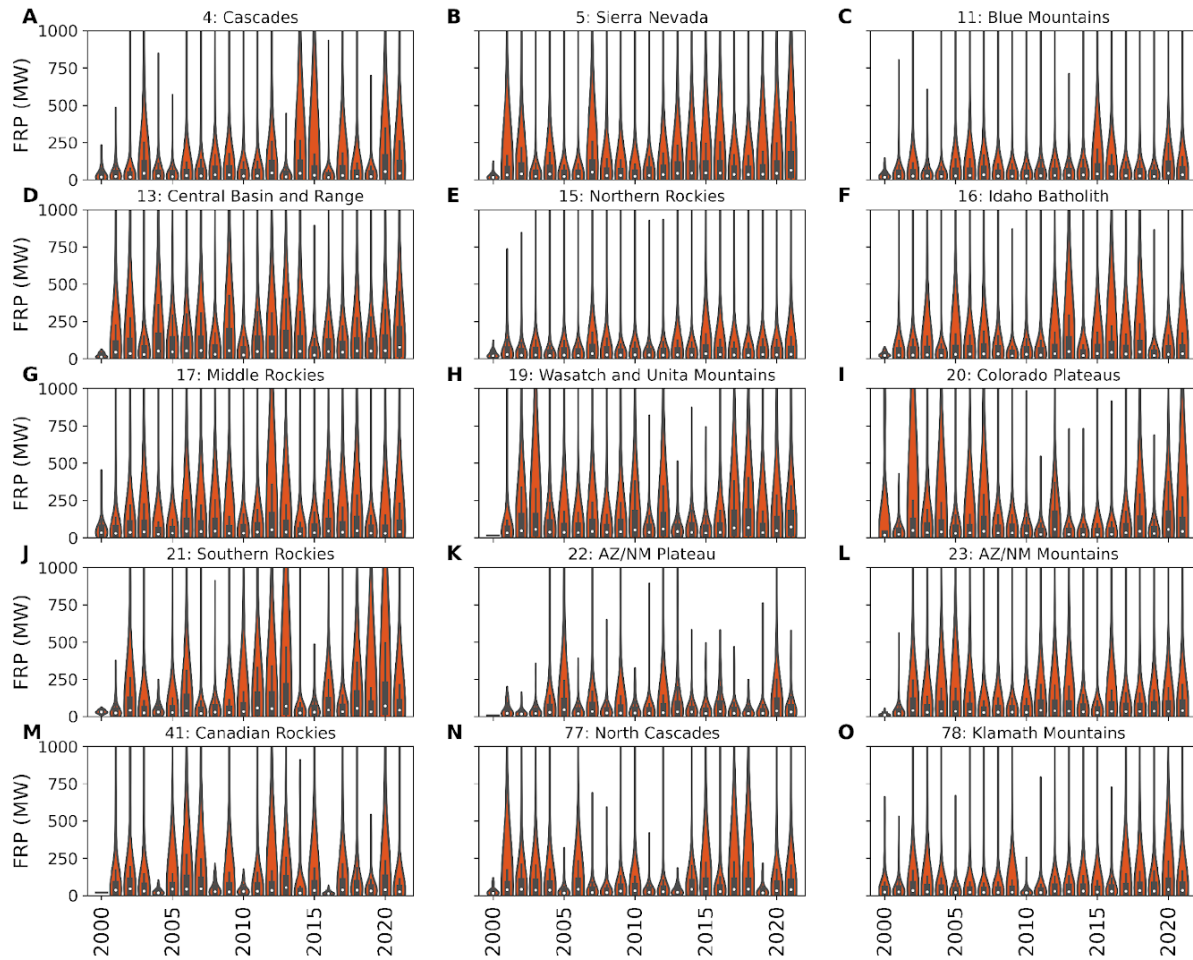


**Figure 4.1 FRP values in each year**

In order to more directly display the linear relationship of FRP over time in these ecoregions, regression plots were graphed. The data was subjected to a Pearson correlation test where the resulting coefficient measures the strength of the association between two continuous variables, such as FRP and time. The ‘r’ coefficient value varies between -1 and +1, with values of 0 implying no correlation, positive values meaning that FRP has an increasing trend over time, and negative values meaning the trendlines are opposite. This test also returns a p-value which represents the probability of the data originating from an uncorrelated system, with values of 0.05 or greater accepting the null hypothesis that FRP and time are uncorrelated (Benesty et al. 2009). Figure 4.2 shows

this data for each ecoregion, with the corresponding trendlines, 'r' coefficient values, and p-values. This figure also plots 95% confidence interval around the linear trend.

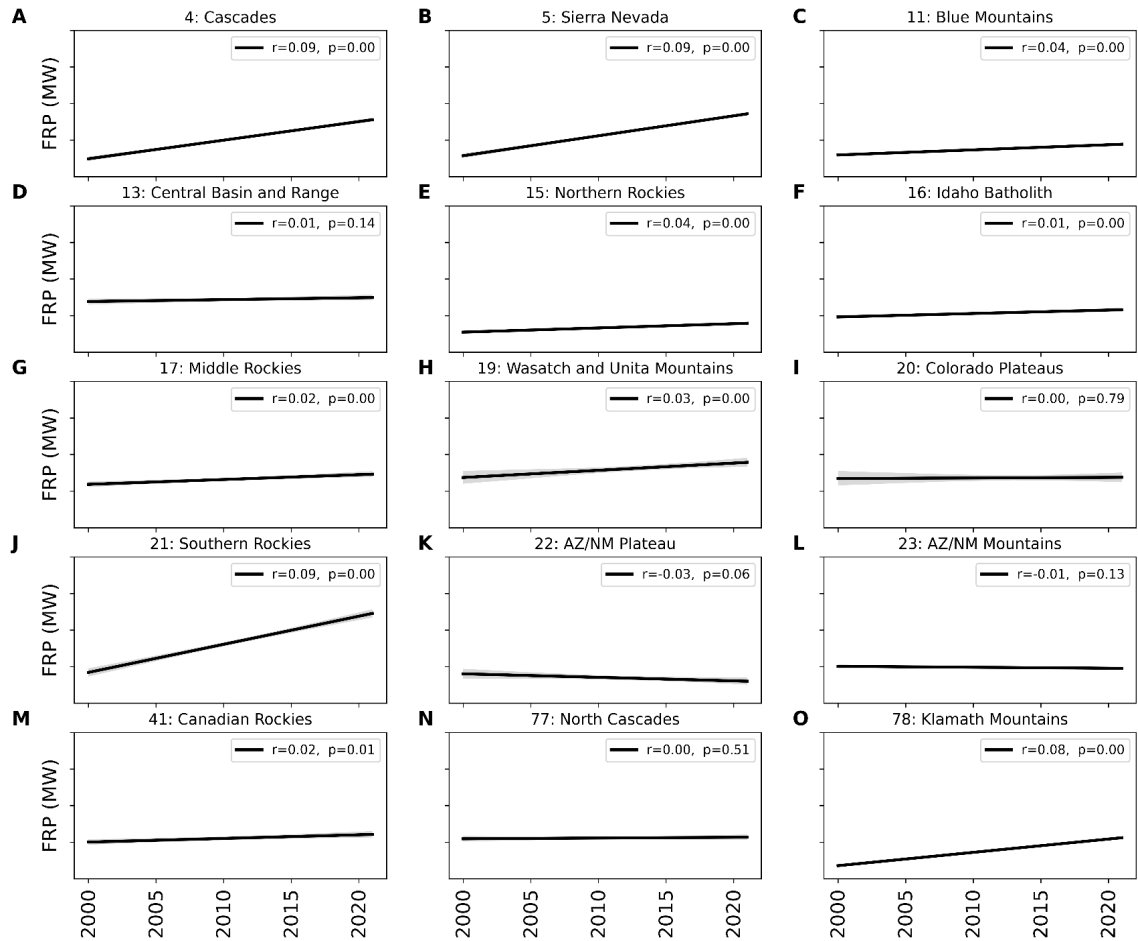


**Figure 4.2 Trends in FRP values as a function of year**

In observing these results, 10 ecoregions had statistically significant increase in FRP as a function of time, 1 ecoregion had statistically non-significant increase in FRP as a function of time, two ecoregions had no trend ( $r = 0$ ), and two ecoregions (Ecoregion 22: Arizona/New Mexico Plateau and Ecoregion 23: Arizona/New Mexico Mountains) were associated with statistically non-significant decreasing trends in FRP over time.

Quantile regression is another way to model the relationship between independent variables, such as FRP, and time. This method displays the specific percentiles, or

quantiles, to estimate a median regression slope (Yu et al. 2003). Figure 4.3 shows this method for all ecoregions. This approach allows for examining trends in various percentiles of FRP with respect to time. Figure 4.3 shows that higher percentiles of FRP are associated with higher increasing rates as a function of time for almost all ecoregions except for Arizona New Mexico Plateau and Mountains (Ecoregion 22 and Ecoregion 23) and North Cascades (Ecoregion 77). This indicates that higher intensity fires in each year are increasing at a higher rate compared to lower intensity fires.

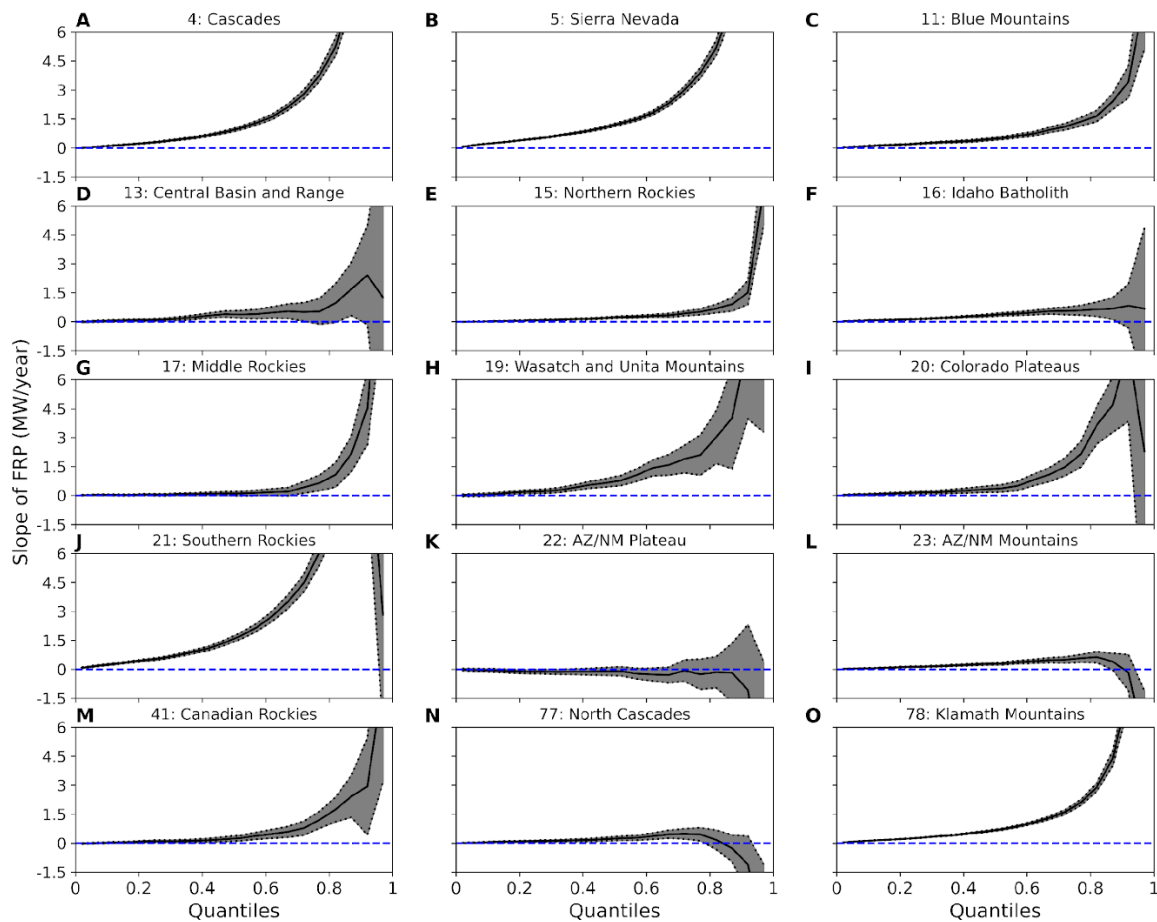


**Figure 4.3** Quantile regression of the slope of FRP values over time



#### 4.4.2 Fire Radiative Power Trends Over Elevation

To display trends in FRP over elevation, FRP values were organized by elevation into seven specific groups: 0 to 500, 500 to 1000, 1000 to 1500, 1500 to 2000, 2000 to 2500, 2500 to 3000, and above 3000 meters. Once arranged, the data was run through Python to plot histograms of FRP with respect to these groups. These plots are useful in viewing the elevational distribution of FRP, and they clearly display the shape, center and spread of the data. Figure 4.4 shows a comparison of this data for each ecoregion.

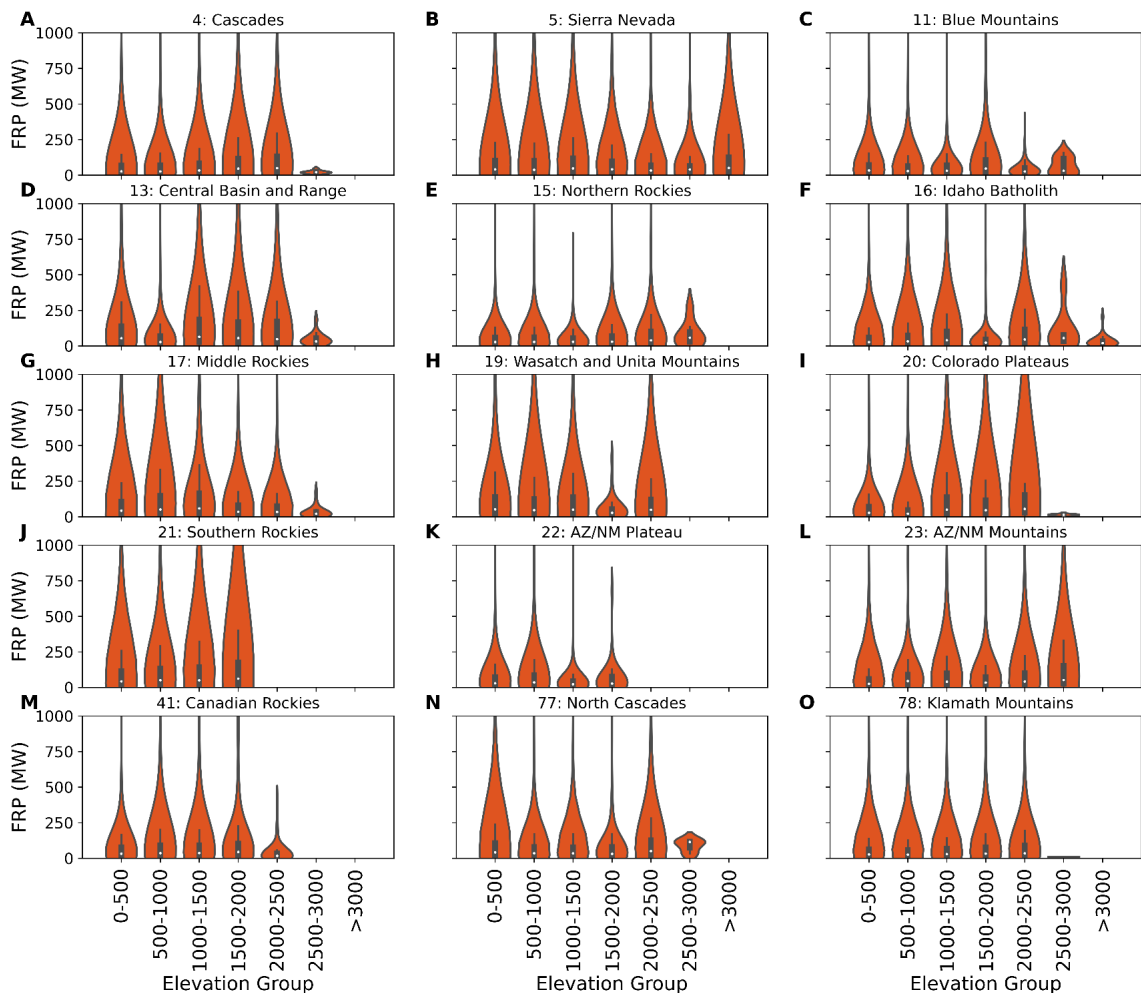


**Figure 4.4** FRP values in each elevation group

Although this figure displays all fire data, some ecoregions do not have data in the 2000 to 2500, 2500 to 3000, or above 3000-meter ranges due to elevation constraints in these regions. For the available data, however, it is clear that a majority of the ecoregions have more intense fires at higher elevations.

To display the linear relationship of FRP in relation to elevation (not elevation group), regression plots were graphed for each ecoregion. Similar to Figure 4.2 displaying the trendline for FRP over time, the data was subjected to a Pearson correlation test which returned a 'r' coefficient and a p-value, however, this test plotted FRP versus elevation. Figure 4.5 shows this data for each ecoregion, with the corresponding trendlines, 'r' coefficient values, and p-values.

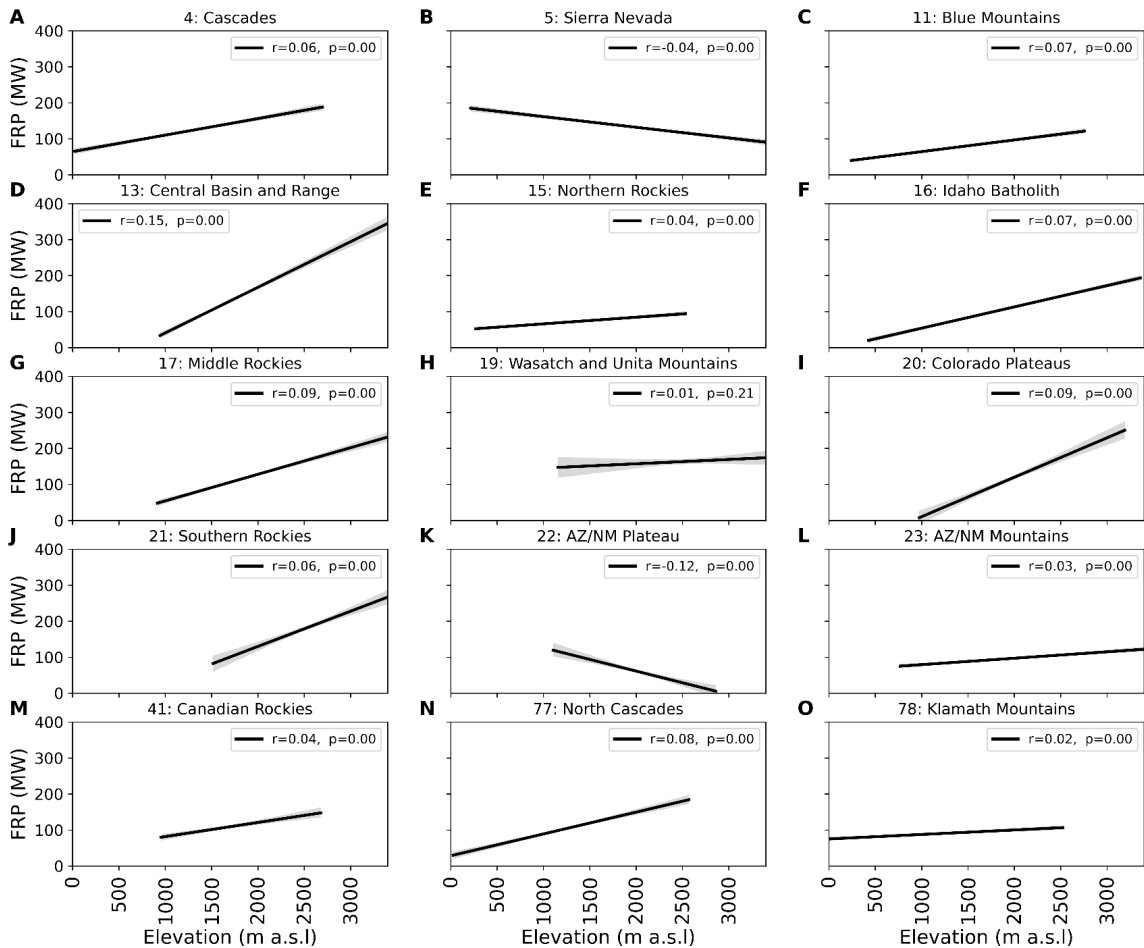


**Figure 4.5 Trends in FRP values versus elevation**

The displayed data shows that all ecoregions besides Ecoregion 5: Sierra Nevada (statistically significant decreasing trend), Ecoregion 19: Wasatch and Unita Mountains (statistically non-significant decreasing trend) and Ecoregion 22: Arizona/New Mexico Plateau (statistically significant decreasing trend) have increasing trends in FRP with elevation gain, and this relationship is statistically significant.

The relationship between FRP and elevation can also be presented using quantile regression. This method displays the quantiles to estimate a median regression slope of FRP with respect to elevation. Figure 4.6 displays this data.

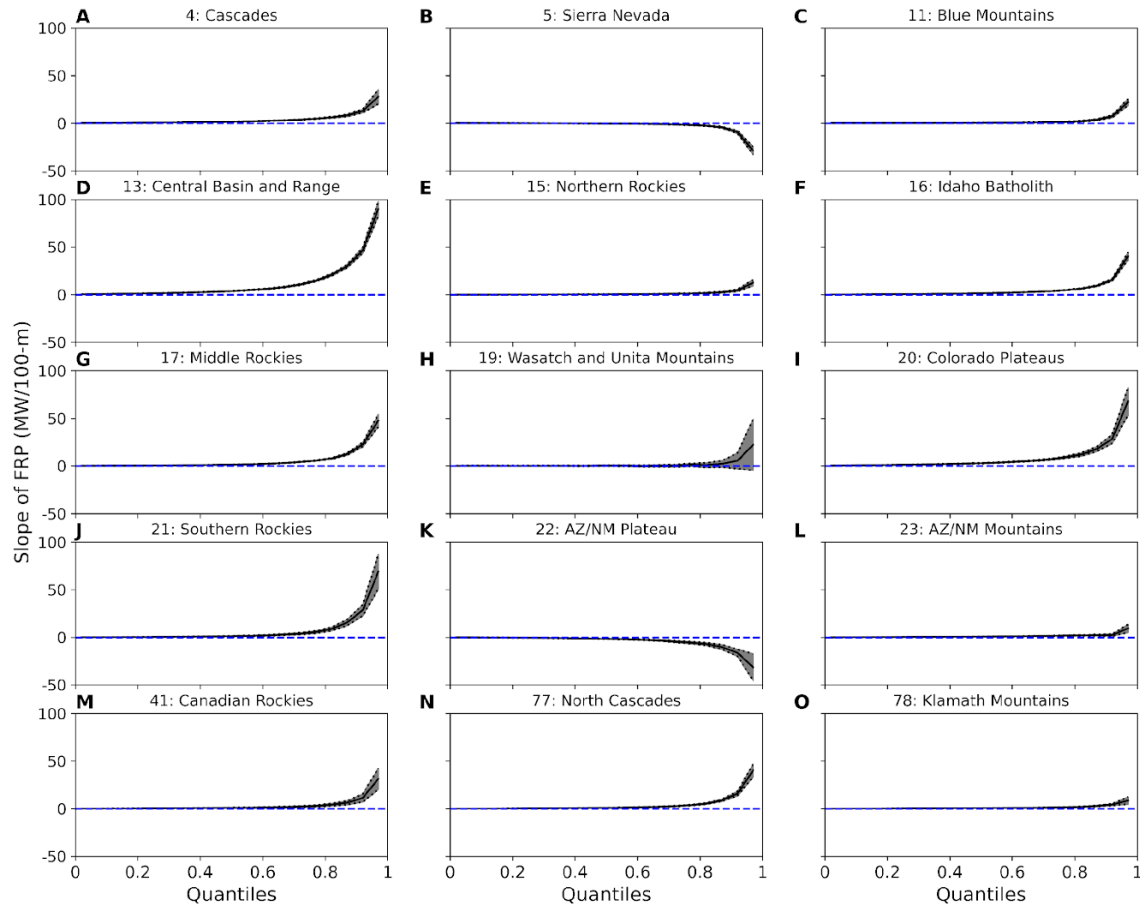


**Figure 4.6** Quantile regression of the slope of FRP values versus elevation

The results of this method exhibit how the higher quantiles are observing greater slopes in FRP at higher elevations in all ecoregions except for Wasatch and Unita Mountains (Ecoregion 19) and Arizona and New Mexico Plateau (Ecoregion 22). This indicates that high-intensity fires are intensifying at a higher rate as a function of elevation compared to low-intensity fires.

#### 4.5 Discussion

By performing ten statistical hypothesis tests and graphical analysis on the data for each ecoregion, we were able to confidently answer the research questions if high-elevation forests burn at a higher intensity than low-elevation forests, and if this

relationship holds across important ecoregions in the western US. We also determined if fires are burning more intensely in recent years compared to the 2000s.

According to the quantitative analysis provided by the statistical tests, trends are evident in the data across almost all ecoregions. Upon splitting the data about the median elevation, it was found that all ecoregions, besides Ecoregion 19: Wasatch and Unita Mountains, had comparatively different means, variances, and distributions between FRP values at high-elevations versus low-elevations.

The graphical analysis also provided a comprehensive comparison between all ecoregions by presenting the results for FRP trends over time and FRP trends over elevation in the West. By taking the form of histograms, trendlines, and quantile regression plots, the figures revealed that trends in FRP increase with elevation gain in nearly all ecoregions besides Ecoregion 5: Sierra Nevada, Ecoregion 22: Arizona/New Mexico Plateau, and Ecoregion 23: Arizona/New Mexico Mountains. This means that fire intensity progresses as wildfires move upslope, supporting the hypothesis that fires are more intense in high-elevation mesic forests than low-elevation forests.

Chapter 5 provides a summary of this thesis work and recommendations for future research.

## CHAPTER 5: SUMMARY

### 5.1 Summary

Wildfires are a naturally occurring process that have long played an extensive role in the health of many of Earth's ecosystems, however, changing wildfire behavior due to climate change threatens to upset the status quo.

The emissions produced by wildfires have one of the largest impacts on global atmospheric composition, climate, and local environmental pollution in many regions globally (Crutzen and Andreae 1990; Garbaras et al. 2015; Guo et al. 2017). Rising temperature levels, shorter winters with earlier spring snowmelt, and increased drought are intensifying wildfire activity in many regions across the world (Flannigan et al. 2009; Huning and AghaKouchak 2020; Rahmstorf et al. 2017). Mega-fires with a much higher burn severity have increased in occurrence, especially in mesic forests where it has previously been too wet to burn frequently (Evers et al. 2021). As these record-breaking wildfires become increasingly common worldwide, we look to the western US where wildfire behavior is just as rampant.

Over the past half-century, trends in burn area, fire size, and the number of large fires have been increasing in the western US, as well as the length of the fire season and the elevation of wildfires (Dennison et al. 2014; Westerling 2016). Particularly in montane environments, there has been an increase in temperature with elevation gain, longer snow-free periods, increased evaporative demand, declines in precipitation during the fire season, and an increase in the number of convective storms and lightning strikes

due to a warming climate (Abatzoglou and Williams 2016; Del Genio et al. 2007; Holden et al. 2018; Pepin et al. 2015; Westerling et al. 2006). These factors contribute to a change in wildfire activity by providing dry fuel in excess during the typical fire season.

Wildfires in the western US have been heavily researched in the past, however, the unprecedented upslope advance of the elevational distribution of these wildfires is a cause for severe concern. Between the years of 1984 and 2017, there has been a median upslope advance of 252 meters in high-elevation forest fires, as well as a median upslope drift of warm season VPD of 295 meters (Alizadeh et al. 2021). This exposes 11% more area (81,500 square kilometers) in western US forests to wildfires that have not seen fire in the modern history, creating the potential to transform montane ecosystems and watersheds in these areas.

When determining how best to fight these fires, forest ecologists, engineers, and fire managers turn to fire behavior models, fire impact assessments, and combustion rate statistics. Fire intensity is an important variable in these tests as it measures the amount of energy emitted by a fire, which correlates to the amount of biomass consumed in the burning process. FRP values are important indicators of wildfires' intensity, since it concerns the amount of radiant energy released by a fire (Costa and Fonseca 2017). These values are obtained via the MODIS sensor aboard the Terra and Aqua satellites, and are used in this research as a proxy for determining the trend in fire intensity as a function of elevation.

The purpose of this study was to test the hypothesis that wildfires burn more intensely in high-elevation mesic forests than in low-elevation dry forests. The research of this thesis involves FRP data for fires between 2000 and 2021, which is paired with

elevation data using digital elevation maps. The data is derived for the 15 mountainous ecoregions of the western US and compiled using ArcGIS Pro into individual FRP-elevation datasets. Various hypothesis tests were then conducted to determine whether or not there is a statistically significant trend in FRP as a function of elevation, and graphical analysis was performed to visually assess the data.

Statistical analysis was performed on the data in the form of ten hypothesis tests. The combination of these tests assessed the relationship between FRP and elevation in the fifteen ecoregions by providing statistics on trends, means, variances, and distributions. Upon examination of the returned statistics, the only tests that accepted the null hypothesis that the means of the fire data samples for low-elevation fires and high-elevation fires are statistically similar were the Student's T-test and ANOVA for Ecoregion 19: Wasatch and Unita Mountains. These results indicate that Ecoregion 19 has the same mean FRP value between high-elevation and low-elevation FRP values split about the fire data point with the median elevation. With the remaining fourteen ecoregions accepting the alternative hypotheses for tests, it can be determined that FRP values in the high-elevation and low-elevation ranges in this study have statistically different means, sample variances, and distributions.

Graphical analysis was also performed in order to visually test the hypothesis that fires at higher elevations burn more intensely. The figures developed from this analysis provided a complete comparison between all ecoregions by presenting the results for FRP trends over time and FRP trends as a function of elevation. Histograms, trendlines, and quantile regression plots showed that trends in FRP increase with elevation gain in nearly all ecoregions besides Ecoregion 5: Sierra Nevada, Ecoregion 22: Arizona/New Mexico



Plateau, and Ecoregion 23: Arizona/New Mexico Mountains. These results signify that fire intensity progresses as wildfires move upslope, thus supporting the hypothesis that fires are more intense in high-elevation mesic forests than low-elevation dry forests, and that this relationship holds across mountainous ecoregions in the western US.

High-elevation wildfires and their intensity have a detrimental effect on societal and ecological systems. They impact terrestrial carbon storage, snowpack, and the quantity and quality of water resources, as well as air pollution, climate, food supply, and biodiversity (Alizadeh et al. 2021; Keeley 2009). Understanding this phenomenon can inform wildfire and land management when the need to address fires in a warming climate is even more pertinent.

## **5.2 Future Research**

The analysis of the hypothesis could be furthered by incorporating tree cover statistics in the fifteen ecoregions specified in this study. By integrating the percentage of forested tree cover in areas that wildfires occurred, the results would provide a more accurate synopsis of the relationship between fire intensity and elevation. For example, Ecoregion 5: Sierra Nevada rises to elevations above treeline where vegetation and tree density decreases due to the underlying granite bedrock. Constricting the data within certain tree cover percentages would allow a more in-depth analysis of FRP as a function of elevation in high-elevation and low-elevation forests.

## REFERENCES

- Abatzoglou, J. T., and A. P. Williams. 2016. "Impact of anthropogenic climate change on wildfire across western US forests." *Proc. Natl. Acad. Sci.*, 113 (42): 11770–11775. <https://doi.org/10.1073/pnas.1607171113>.
- Alizadeh, M. R., J. T. Abatzoglou, C. H. Luce, J. F. Adamowski, A. Farid, and M. Sadegh. 2021. "Warming enabled upslope advance in western US forest fires." *Proc. Natl. Acad. Sci.*, 118 (22): e2009717118. <https://doi.org/10.1073/pnas.2009717118>.
- ArcGIS Pro. 2022. "About ArcGIS Pro." *ESRI*. <https://pro.arcgis.com/en/pro-app/2.8/get-started/get-started.htm> (September 12, 2021).
- Arsham, Hossein, and Miodrag Lovric. 2011. "Bartlett's Test." *International encyclopedia of statistical science* 87-88.
- Baker, W. L. 1993. "Spatially Heterogeneous Multi-Scale Response of Landscapes to Fire Suppression." *Oikos*, 66 (1): 66. <https://doi.org/10.2307/3545196>.
- Balch, J. K., B. A. Bradley, J. T. Abatzoglou, R. C. Nagy, E. J. Fusco, and A. L. Mahood. 2017. "Human-started wildfires expand the fire niche across the United States." *Proc. Natl. Acad. Sci.*, 114 (11): 2946–2951. <https://doi.org/10.1073/pnas.1617394114>.
- Barrett, K., and E. S. Kasischke. 2013. "Controls on variations in MODIS fire radiative power in Alaskan boreal forests: Implications for fire severity conditions." *Remote Sens. Environ.*, 130: 171–181. <https://doi.org/10.1016/j.rse.2012.11.017>.
- Barry, R. G. 1992. "Mountain Climatology and Past and Potential Future Climatic Changes in Mountain Regions: A Review." *Mt. Res. Dev.*, 12 (1): 71. <https://doi.org/10.2307/3673749>.

- Benesty, J., J. Chen, Y. Huang, and I. Cohen. 2009. "Pearson Correlation Coefficient." *Noise Reduct. Speech Process.*, Springer Topics in Signal Processing, 1–4. Berlin, Heidelberg: Springer Berlin Heidelberg.
- Berger, C., Grand, L., Fitzgerald, S.A., Leavell, D. 2018. "What is fire severity?" EM9222, Extension & Experiment Station Communications, Oregon State University. 2p.
- Binkley, D., T. Sisk, C. Chambers, J. Springer, and W. Block. 2007. "The Role of Old-growth Forests in Frequent-fire Landscapes." *Ecol. Soc.*, 12 (2): art18. <https://doi.org/10.5751/ES-02170-120218>.
- Conover, W. J., M. E. Johnson, and M. M. Johnson. 1981. "A Comparative Study of Tests for Homogeneity of Variances, with Applications to the Outer Continental Shelf Bidding Data." *Technometrics*, 23 (4): 351–361. <https://doi.org/10.1080/00401706.1981.10487680>.
- Cooper, C. F. 1960. "Changes in Vegetation, Structure, and Growth of Southwestern Pine Forests since White Settlement." *Ecol. Monogr.*, 30 (2): 129–164. <https://doi.org/10.2307/1948549>.
- Corder, G. W., and D. I. Foreman. 2014. "Nonparametric statistics: a step-by-step approach." *Wiley*, Hoboken, New Jersey.
- Costa, B. S. C. da, and E. L. da Fonseca. 2017. "The Use of Fire Radiative Power to Estimate the Biomass Consumption Coefficient for Temperate Grasslands in the Atlantic Forest Biome." *Rev. Bras. Meteorol.*, 32 (2): 255–260. <https://doi.org/10.1590/0102-77863220004>.
- Crutzen, P. J., and M. O. Andreae. 1990. "Biomass Burning in the Tropics: Impact on Atmospheric Chemistry and Biogeochemical Cycles." *Science*, 250 (4988): 1669–1678. <https://doi.org/10.1126/science.250.4988.1669>.
- D'Agostino, R. B., A. Belanger, and R. B. D'Agostino. 1990. "A Suggestion for Using Powerful and Informative Tests of Normality." *Am. Stat.*, 44 (4): 316. <https://doi.org/10.2307/2684359>.

- Dale, L. 2006. "Wildfire Policy and Fire Use on Public Lands in the United States." *Soc. Nat. Resour.*, 19 (3): 275–284. <https://doi.org/10.1080/08941920500460898>.
- Del Genio, A. D., M.-S. Yao, and J. Jonas. 2007. "Will moist convection be stronger in a warmer climate?: CONVECTION STRENGTH IN A WARMER CLIMATE." *Geophys. Res. Lett.*, 34 (16). <https://doi.org/10.1029/2007GL030525>.
- Dennison, P. E., S. C. Brewer, J. D. Arnold, and M. A. Moritz. 2014. "Large wildfire trends in the western United States, 1984-2011: DENNISON ET. AL.; LARGE WILDFIRE TRENDS IN THE WESTERN US." *Geophys. Res. Lett.*, 41 (8): 2928–2933. <https://doi.org/10.1002/2014GL059576>.
- Dickey, D. A., and W. A. Fuller. 1979. "Distribution of the Estimators for Autoregressive Time Series With a Unit Root." *J. Am. Stat. Assoc.*, 74 (366): 427. <https://doi.org/10.2307/2286348>.
- Easterling, D. R., J. R. Arnold, T. Knutson, K. E. Kunkel, A. N. LeGrande, L. R. Leung, R. S. Vose, D. E. Waliser, and M. F. Wehner. 2017. *Ch. 7: Precipitation Change in the United States. Climate Science Special Report: Fourth National Climate Assessment, Volume I*. U.S. Global Change Research Program.
- Evers, C., S. Busby, M. Nielsen-Pincus, and A. Holz. 2021. *Extreme Winds Flip Influence of Fuels and Topography on Megafire Burn Severity in Mesic Conifer Forests Under Record Fuel Aridity*. preprint. In Review.
- Ferguson, R. L., D. M. Galuszka, T. M. Hare, D. P. Mayer, and B. L. Redding. 2020. "Mars 2020 Terrain Relative Navigation HiRISE Orthorectified Image Mosaic." U.S. Geological Survey.
- Flannigan, M., B. Stocks, M. Turetsky, and M. Wotton. 2009. "Impacts of climate change on fire activity and fire management in the circumboreal forest." *Glob. Change Biol.*, 15 (3): 549–560. <https://doi.org/10.1111/j.1365-2486.2008.01660.x>.
- Fuller, W. A. 1976. *Introduction to statistical time series*. A Wiley publication in applied statistics. New York: Wiley.

- Garbaras, A., A. Masalaite, I. Garbariene, D. Ceburnis, E. Krugly, V. Remeikis, E. Puida, K. Kvietkus, and D. Martuzevicius. 2015. "Stable carbon fractionation in size-segregated aerosol particles produced by controlled biomass burning." *J. Aerosol Sci.*, 79: 86–96. <https://doi.org/10.1016/j.jaerosci.2014.10.005>.
- Giglio, L. 2000. "MODIS Thermal Anomalies/Fire Products." NASA Land Atmosphere Near real-time Capability for EOS Fire Information for Resource Management System.
- Giglio, L., J. Descloitres, C. O. Justice, and Y. J. Kaufman. 2003. "An Enhanced Contextual Fire Detection Algorithm for MODIS." *Remote Sens. Environ.*, 87 (2–3): 273–282. [https://doi.org/10.1016/S0034-4257\(03\)00184-6](https://doi.org/10.1016/S0034-4257(03)00184-6).
- Griffin, Jonathon. 2021. "New Timeline of Deadliest California Wildfire Could Guide Lifesaving Research and Action." *National Institute of Standards and Technology* <https://www.nist.gov/news-events/news/2021/02/new-timeline-deadliest-california-wildfire-could-guide-lifesaving-research> (March 13, 2022).
- Guo, M., J. Li, J. Xu, X. Wang, H. He, and L. Wu. 2017. "CO<sub>2</sub> emissions from the 2010 Russian wildfires using GOSAT data." *Environ. Pollut.*, 226: 60–68. <https://doi.org/10.1016/j.envpol.2017.04.014>.
- Hartmann, K., Krois, J., Waske, B. (2018): E-Learning Project SOGA: Statistics and Geospatial Data Analysis. *Department of Earth Sciences, Freie Universitaet Berlin* <https://www.geo.fu-berlin.de/en/v/soga/index.html> (April 24, 2022).
- Herrando, S., and L. Brotons. 2002. "Forest bird diversity in Mediterranean areas affected by wildfires: a multi-scale approach." *Ecography*, 25 (2): 161–172. <https://doi.org/10.1034/j.1600-0587.2002.250204.x>.
- Holden, Z. A., A. Swanson, C. H. Luce, W. M. Jolly, M. Maneta, J. W. Oyler, D. A. Warren, R. Parsons, and D. Affleck. 2018. "Decreasing fire season precipitation increased recent western US forest wildfire activity." *Proc. Natl. Acad. Sci.*, 115 (36). <https://doi.org/10.1073/pnas.1802316115>.

- Huning, L. S., and A. AghaKouchak. 2020. "Global snow drought hot spots and characteristics." *Proc. Natl. Acad. Sci.*, 117 (33): 19753–19759.  
<https://doi.org/10.1073/pnas.1915921117>.
- Jain, T. B., and R. T. Graham. 2015. *Restoring Dry and Moist Forests of the Inland Northwestern United States*.
- Keeley, J. E. 2009. "Fire intensity, fire severity and burn severity: a brief review and suggested usage." *Int. J. Wildland Fire*, 18 (1): 116.  
<https://doi.org/10.1071/WF07049>.
- Khorshidi, M.S., Dennison, P.E., Nikoo, M.R., AghaKouchak, A., Luce, C.H. and Sadegh, M. 2020. "Increasing concurrence of wildfire drivers tripled megafire critical danger days in Southern California between 1982 and 2018." *Environmental Research Letters*, 15(10), p.104002.
- Laurent, P., F. Mouillot, M. V. Moreno, C. Yue, and P. Ciais. 2019. "Varying relationships between fire radiative power and fire size at a global scale." *Biogeosciences*, 16 (2): 275–288. <https://doi.org/10.5194/bg-16-275-2019>.
- Lewis, D. 2020. "'Deathly silent': Ecologist describes Australian wildfires' devastating aftermath." *Nature*, 577 (7790): 304.
- Levy, R. C., S. Mattoo, V. Sawyer, Y. Shi, P. R. Colarco, A. I. Lyapustin, Y. Wang, and L. A. Remer. 2018. "Exploring systematic offsets between aerosol products from the two MODIS sensors." *Atmos. Meas. Tech.*, 11 (7): 4073–4092.  
<https://doi.org/10.5194/amt-11-4073-2018>.
- Liu, Y., J. Stanturf, and S. Goodrick. 2010. "Trends in global wildfire potential in a changing climate." *For. Ecol. Manag.*, 259 (4): 685–697.  
<https://doi.org/10.1016/j.foreco.2009.09.002>.
- MacFarland, T. W., and J. M. Yates. 2016. "Kruskal–Wallis H-Test for Oneway Analysis of Variance (ANOVA) by Ranks." *Introd. Nonparametric Stat. Biol. Sci. Using R*, 177–211. Cham: Springer International Publishing.

- McMahon, G., S. M. Gregonis, S. W. Waltman, J. M. Omernik, T. D. Thorson, J. A. Freeouf, A. H. Rorick, and J. E. Keys. 2001. "Developing a Spatial Framework of Common Ecological Regions for the Conterminous United States." *Environ. Manage.*, 28 (3): 293–316. <https://doi.org/10.1007/s0026702429>.
- National Park Service. 2021. "Cameron Peak and East Troublesome Fires." <https://www.nps.gov/romo/learn/2020fire.htm> (March 12, 2022).
- Natole, M., Y. Ying, A. Buyantuev, M. Stessin, V. Buyantuev, and A. Lapenis. 2021. "Patterns of mega-forest fires in east Siberia will become less predictable with climate warming." *Environ. Adv.*, 4: 100041. <https://doi.org/10.1016/j.envadv.2021.100041>.
- NOAA National Centers for Environmental information, Climate at a Glance: Regional Time Series. 2020. <https://www.ncdc.noaa.gov/cag/> (March 12, 2022).
- Omernik, J. M. 1987. "Ecoregions of the Conterminous United States." *Ann. Assoc. Am. Geogr.*, 77 (1): 118–125. <https://doi.org/10.1111/j.1467-8306.1987.tb00149.x>.
- Pechony, O., and D. T. Shindell. 2010. "Driving forces of global wildfires over the past millennium and the forthcoming century." *Proc. Natl. Acad. Sci.*, 107 (45): 19167–19170. <https://doi.org/10.1073/pnas.1003669107>.
- Pepin, N., R. S. Bradley, H. F. Diaz, M. Baraer, and E. B. Caceres. 2015. "Elevation-dependent warming in mountain regions of the world." *Nat. Clim. Change*, 5 (5): 424–430. <https://doi.org/10.1038/nclimate2563>.
- Rahmstorf, S., G. Foster, and N. Cahill. 2017. "Global temperature evolution: recent trends and some pitfalls." *Environ. Res. Lett.*, 12 (5): 054001. <https://doi.org/10.1088/1748-9326/aa6825>.
- Remke, M.J., Chambers, M.E., Tuten, M.C, Pelz, K.A. 2021. "Mixed Conifer Forests in the San Juan Mountain Region of Colorado, USA: The Status of Our Knowledge and Management Implications." *Colorado Forest Restoration Institute*. CFRI-2110

Ruefenacht, B., M. V. Finco, M. D. Nelson, R. Czaplewski, E. H. Helmer, J. A. Blackard, G. R. Holden, A. J. Lister, D. Salajanu, D. Weyermann, and K. Winterberger. 2008. "Conterminous U.S. and Alaska Forest Type Mapping Using Forest Inventory and Analysis Data." *Photogramm. Eng. Remote Sens.*, 74 (11): 1379–1388. <https://doi.org/10.14358/PERS.74.11.1379>.

Rush, Lindsey. 2020. *Bureau of Land Management*.  
<https://www.flickr.com/photos/nifc/51685355383/in/album-72157720147219653/>  
(March 20, 2022).

Sadegh, Mojtaba; Abatzoglou, John; and Alizadeh, Mohammad Reza. 2021. "Western Fires are Burning Higher in the Mountains at Unprecedented Rates: It's a Clear Sign of Climate Change". *The Conversation*  
[https://scholarworks.boisestate.edu/cgi/viewcontent.cgi?article=1172&context=civileng\\_facpubs](https://scholarworks.boisestate.edu/cgi/viewcontent.cgi?article=1172&context=civileng_facpubs) (April 23, 2022).

Seiler, W., and P. J. Crutzen. 1980. "Estimates of gross and net fluxes of carbon between the biosphere and the atmosphere from biomass burning." *Clim. Change*, 2 (3): 207–247. <https://doi.org/10.1007/BF00137988>.

Shapiro, S. S., and M. B. Wilk. 1965. "An Analysis of Variance Test for Normality (Complete Samples)." *Biometrika*, 52 (3/4): 591. <https://doi.org/10.2307/2333709>.

Stephens, S. L., and L. W. Ruth. 2005. "FEDERAL FOREST-FIRE POLICY IN THE UNITED STATES." *Ecol. Appl.*, 15 (2): 532–542. <https://doi.org/10.1890/04-0545>.

Talucci, A. C., M. M. Loranty, and H. D. Alexander. 2022. "Siberian taiga and tundra fire regimes from 2001–2020." *Environ. Res. Lett.*, 17 (2): 025001.  
<https://doi.org/10.1088/1748-9326/ac3f07>.

United Nations Environment Programme. 2022. "Spreading like Wildfire – The Rising Threat of Extraordinary Landscape Fires." *A UNEP Rapid Response Assessment*. Nairobi.

United States Drought Monitor. 2022. "Map Archive." *National Drought Mitigation Center*. <https://droughtmonitor.unl.edu> (March 14, 2022)



- United States Environmental Protection Agency. 2022. “Level III and IV Ecoregions of the Continental United States.” <https://www.epa.gov/eco-research/level-iii-and-iv-ecoregions-continental-united-states> (October 14, 2021).
- United States Geological Survey. 2022. “The National Map.” *National Geospatial Program* <https://www.usgs.gov/programs/national-geospatial-program/national-map> (October 25, 2021).
- Westerling, A. L. 2016. “Increasing western US forest wildfire activity: sensitivity to changes in the timing of spring.” *Philos. Trans. R. Soc. B Biol. Sci.*, 371 (1696): 20150178. <https://doi.org/10.1098/rstb.2015.0178>.
- Westerling, A. L., H. G. Hidalgo, D. R. Cayan, and T. W. Swetnam. 2006. “Warming and Earlier Spring Increase Western U.S. Forest Wildfire Activity.” *Science*, 313 (5789): 940–943. <https://doi.org/10.1126/science.1128834>.
- Wooster, M. J., G. Roberts, G. L. W. Perry, and Y. J. Kaufman. 2005. “Retrieval of biomass combustion rates and totals from fire radiative power observations: FRP derivation and calibration relationships between biomass consumption and fire radiative energy release.” *J. Geophys. Res.*, 110 (D24): D24311. <https://doi.org/10.1029/2005JD006318>.
- Yazici, B., and S. Yolacan. 2007. “A comparison of various tests of normality.” *Journal of Statistical Computation and Simulation*, 77 (2): 175–183. <https://doi.org/10.1080/10629360600678310>.
- Yu, K., Z. Lu, and J. Stander. 2003. “Quantile regression: applications and current research areas.” *J. R. Stat. Soc. Ser. Stat.*, 52 (3): 331–350. <https://doi.org/10.1111/1467-9884.00363>.
- Ziel, Robert. 2020. *Bureau of Land Management*. <https://www.flickr.com/photos/nifc/50138885702/in/album-72157715188792528/> (March 20, 2022).